2005:117 CIV

EXAMENSARBETE

Development of a MatLab-based GPS Constellation Simulation for Navigation Algorithm Developments

PER GUSTAVSSON

MASTER OF SCIENCE PROGRAMME
in Space Engineering

Luleå University of Technology
Department of Space Science, Kiruna

LULEÅ TEKNISKA UNIVERSITET

2005:117 CIV • ISSN: 1402 - 1617 • ISRN: LTU - EX - - 05/117 - - SE

Development of a Matlab-based GPS-constellation simulation for navigation algorithm developments

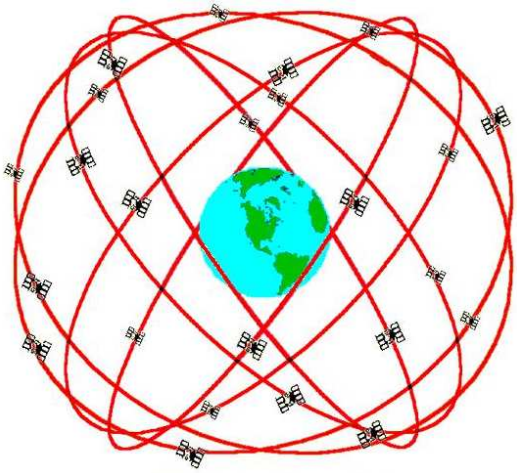

Written:	Per Gustavsson	Date:	2005-03-10
Approved:	Dr. Stephan Theil	Date:	2005-03-10
Approved:	Dr. Priya Fernando	Date:	2005-04-08

Abstract

This thesis is a part of a PhD project called *Algorithm for Coupled Navigation Using an Inertial Measurement Unit and the Global Positioning System*. The aim of the PhD project is to study a continuous navigation and attitude update solution and its applicability to several aeronautical and space missions.

In this thesis a software-based GPS receiver simulator for the L1 C/A code signal is developed and verified. The simulator is implemented in MATLAB although most functions are coded in C to accelerate the speed of operation. A mathematical model is developed to express the *Pseudo Range* as a function of various errors, such as satellite clock error, ionospheric error, and tropospheric error. The simulation program is developed so the receiver could be spaceborne, which means that special situations have been implemented in models for GPS satellite visibility, ionospheric and tropospheric time delay effects.

The verification of the developed simulation program was performed by comparing simulated parameters with calculated hardware code parameters from a real receiver, using same input. The result was satisfied and following differences could be seen:

Calculated GPS Time $< 1.3 \cdot 10^{-7}\ s$

Geometric Range $< 1 \cdot 10^{-2}\ m$

Ionospheric Range Error $< 4\ m$

Tropospheric Range Error $< 0.6\ m$

Satellite Clock Range $< 0.2\ m$

Foreword

This report is submitted to the Department of Space Science in partial fulfilment of the requirements for the degree of Master of Science in Space Engineering at Luleå University of Technology, Sweden. The work was carried out in the Space Technology group at the Center of Applied Space Technology and Microgravity (ZARM) at the University of Bremen, Germany.

I thank my supervisors, Dr. Stephan Theil and PhD student Gustavo Baldo Carvalho, for the opportunity to make my thesis at ZARM and for giving me great support and guiding through my work. Without Gustavo's eagle eyes on finding errors the result of this thesis would not be the same. I would also like to thank Silvia Scheithauer for helping me through administrative matters associated with working in Germany and my Swedish supervisor Dr. Priya Fernando who has given me insight in the space business. At last I would like to thank my family, for supporting me during my student years and with my constant moving around.

Contents

List of Figures

List of Tables

Indexing and Abbreviations

Indexing

The following conventions are used:

- The superscript means the reference frame to which the physical entity is described. Ex.: $\underline{r}^i$ means the vector $\underline{r}$ described in the reference frame i.
- The subscript and superscript together means a transformation or attitude between two reference frames.
  Ex.: $\underline{\underline{T}}_b^i$ means the transformation matrix, which takes a vector described in the reference frame b and transforms it into a vector described in the reference frame i.
- Two subscripts and one superscript together means the attitude rate description between both subscript reference frames described in the superscript reference frame.
  Ex.: $\underline{\omega}_{i,b}^b$ means attitude rate $\underline{\omega}$ of reference frame b related to reference frame i described in the reference frame b.
- The signs of rotations within the frames are defined by the right hand rule.

Abbreviations

BPSK	Binary Phase Shift Keying, a modulation technique.
C/A code	The standard (Coarse/Acquisition) GPS PRN code, also known as the Civilian Code. Only modulated on the L1 carrier.
Clock Bias	The difference between the receiver or satellite clock's indicated time
DGPS	Differential GPS
DOP	Dilution of Precision. An indicator of satellite geometry for a unique constellation of satellites used to determine a position.
ECEF	Earth Centered, Earth Fixed
ECI	Earth Centered Inertial
ENU	East North Up
GPS	Global Positioning System
HOW	Hand-Over Word
L1	Is the 1575.42MHz GPS carrier frequency which contains the C/A-Code, the encrypted P-Code and the Navigation Message.
MCS	Master Control Station
NAV	Navigation
NED	North East Down
PRN	Pseudo Random Noise
RF	Radio Frequency
SNR	Signal to Noise Ratio
SV	Satellite vehicle (the GPS satellite)
TLM	Telemetry word
UHF	Ultra High Frequency
UTC	Universal Time Coordinated
WAAS	Wide Area Augmentation System

1. Introduction

The navigation system is one of the most important spacecraft sub-systems. It satisfies two tasks: On one hand the navigation system has to manage the various associated sensors, which provide measurements of the present flight conditions. On the other hand it must supply continuously a navigation solution that can enable the spacecraft to reach and hold some flight conditions required by its mission. A navigation system consists of sensors measuring the current flight conditions, and a navigation software, which estimates flight conditions. This process is called *data fusion*. The main result of this process is a navigation solution that can meet the mission navigation requirements with a precision that could not be achieved using only the available sensors. One of the most used navigation sensors is the GPS (Global Positioning system) receiver. This sensor measures the three-dimensional user present position within the $ECEF$ (Earth-Centered Earth-Fixed) reference frame. This sensor receives signals from the GPS constellation which is constituted of many GPS satellites placed in different orbits. Due to the fact that the GPS constellation orbits are well known, and thus the GPS satellites positions, the user present position can be computed using the incoming GPS signals. These signals are affected by various environmental impacts in such a way that the introduced errors and deviations can lead to a wrong position computation which will affect directly the navigation solution provided by the navigation software.

This thesis is a part of a PhD project called *Algorithm for Coupled Navigation Using an Inertial Measurement Unit and the Global Positioning System*. The aim of the PhD project is to study a continuous navigation and attitude update solution and its applicability to several aeronautical and space missions. A special attention is devoted to **ASTRA** project (Advanced Systems and Technologies for Re-usable launch vehicle Applications). An example within the frame of **ASTRA** is the flight experiment called **PHOENIX** which used navigation algorithm in a blended IMU+GPS system. The algorithm for this system was stated as an extended Kalman filter, which estimates navigation, attitude, dominant IMU (Inertial Measurement Unit) sensor errors and GPS (Global Positioning System) receiver clock errors on a navigating spacecraft during launch, orbit, re-entry and automatic landing phases.

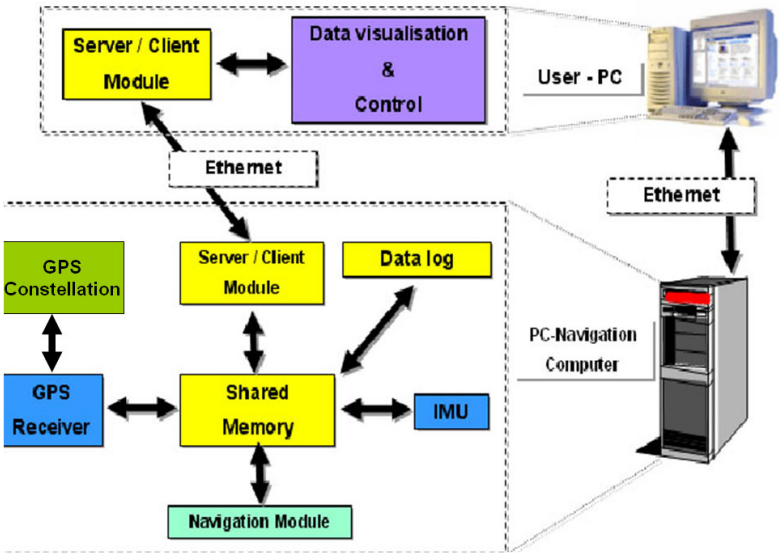

Figure 1: System design of PhD project. This thesis represent the 'GPS Constellation' box.

1.1. Thesis task

Within the scope of this master thesis, a Matlab-based software for GPS constellation simulation with its associated signal errors and deviation effects shall be developed. The development will be guided by the necessities of the work currently carried out at ZARM where the spacecraft navigation subject is in development.

Work to be done

- Review of the currently available GPS bibliography.
- Survey on models for GPS satellite orbit simulation.
- Design and programming of a simulation model for GPS satellite orbit simulation.
- Survey on GPS signal error sources.
- Survey on models for GPS signal error source simulation.
- Modelling of a GPS receiver (no modelling of signal and data processing is required).
- Design and programming of a simulation model for GPS signal error source simulation.
- Software verification and documentation.
  All models shall be programmed in Matlab/C-code

2. GPS information

The Global Positioning System (GPS) is a satellite-based navigation system made up of a network of at least 24 satellites (today 30 in orbit) which has been placed into orbit by the U.S. Department of Defense. GPS was originally intended for military applications, but in 1984 made the U.S. government the system available for civilian. The accuracy may be different but the GPS works in any Earth weather conditions, anywhere in the world, 24 hours a day. The GPS is based on three segments: Space, Control and User segment.

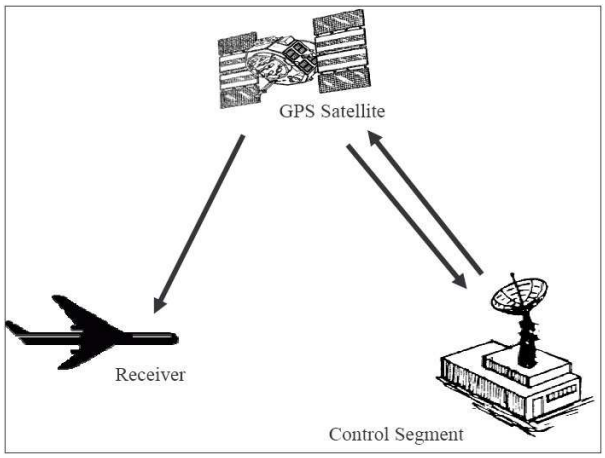

Figure 2: GPS Segments

2.1. Space Segment

The first GPS satellite was launched in 1978 and a full constellation of 24 satellites was achieved in 1994. The orbit altitude is such that the satellites repeat the same ground track each 24 hours. There are six orbital planes (with nominally four SVs in each), equally spaced (60 degrees apart), and inclined at about 55° with respect to the equatorial plane. Each satellite is built to last about 10-15 years. Replacements are constantly being built and launched into orbit. A GPS satellite weighs approximately 900kg and is about 5 meter across with the solar panels extended. Transmitter power is only 50 watts or less.

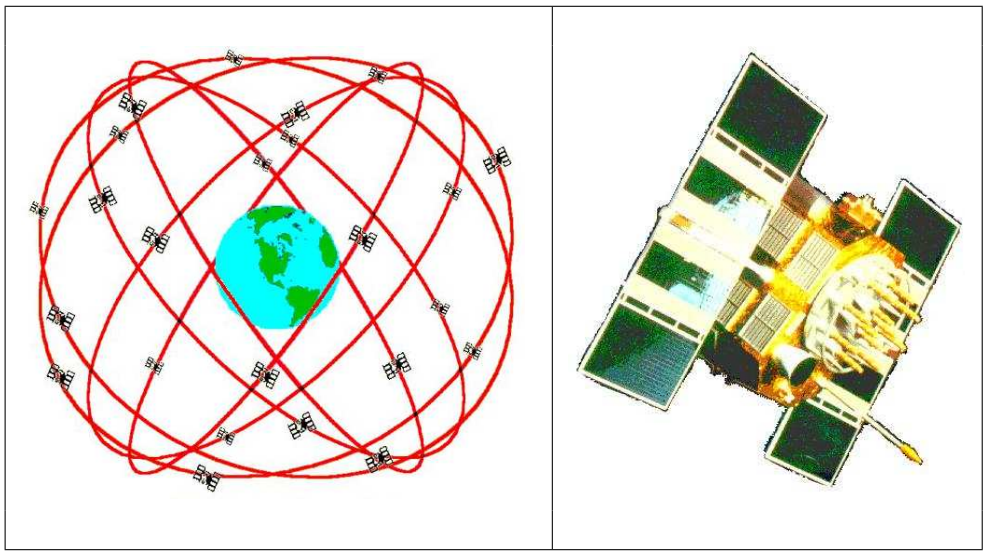

Figure 3: GPS Constellation.

2.2. Control Segment

The GPS Control Segment is comprised of four major components: a Master Control Station (MCS), Backup Master Control Station , four ground antennas, and six monitor stations. The MCS is responsible for all aspects of constellation command and control. Example of this are: Satellite maintenance and anomaly resolution, navigation data upload operations as required to sustain performance in accordance with accuracy performance standards. The six monitor stations provide near real-time satellite ranging measurement data to the MCS and support near-continuous monitoring of constellation performance. The following figure shows the GPS monitoring stations all over the world:

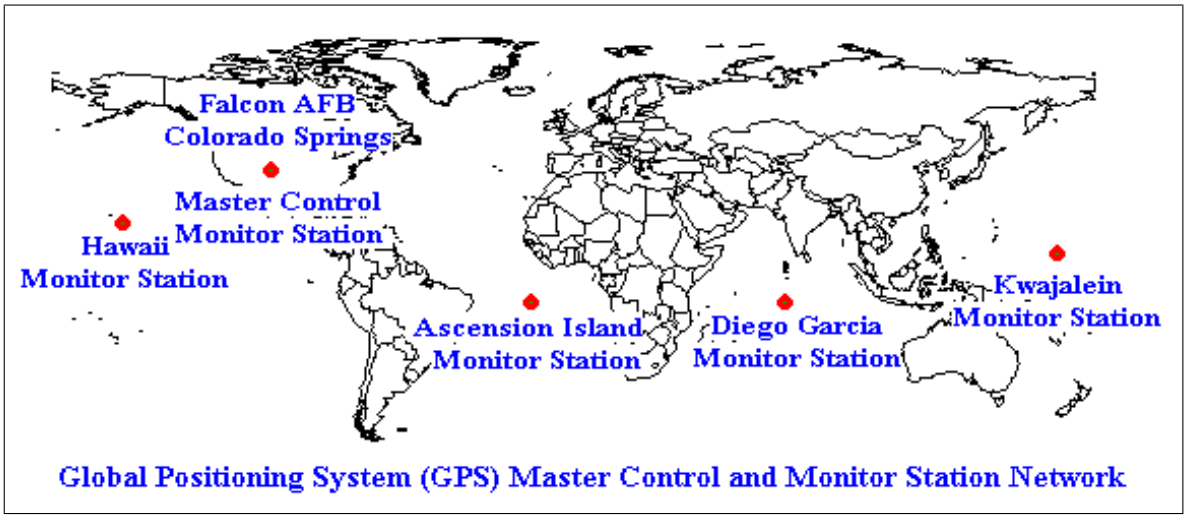

Figure 4: GPS Control Segment.

2.3. User Segment

The user segment consists of the GPS receivers around the world. These receivers get the GPS signals coming from space to provide the position, velocity and time of the user, all related to the Earth-Centered Earth-fixed (ECEF) frame. Some of the GPS applications are:

- Navigation in three dimensions is the primary function of GPS. Navigation receivers are made for aircraft, ships, ground vehicles, and for personal hand-carrying.
- Precise positioning is possible using GPS receivers at reference locations providing corrections and relative positioning data for remote receivers. Surveying, geodetic control, and plate tectonic studies are examples.
- Time and frequency dissemination, based on the precise clocks on board the SVs and controlled by the monitor stations, is another use for GPS. Astronomical observatories, telecommunications facilities, and laboratory standards can be set to precise time signals or controlled to accurate frequencies by special purpose GPS receivers.

2.4. Receiver information

A GPS receiver must be locked on to the signal of at least three GPS satellites to calculate a 2D position (latitude and longitude), which is obtained by triangulation (see figure 5). Essentially, the GPS receiver compares the time a signal was transmitted by a GPS satellite with the time it was received. The time difference tells the GPS receiver how far away the satellite is. With locked signal to four or more satellites (distance measurements), the receiver can determine the user's 3D position (latitude, longitude and altitude). Once the user's position has been determined, the GPS unit can calculate other information, such as speed, bearing, track, etc.

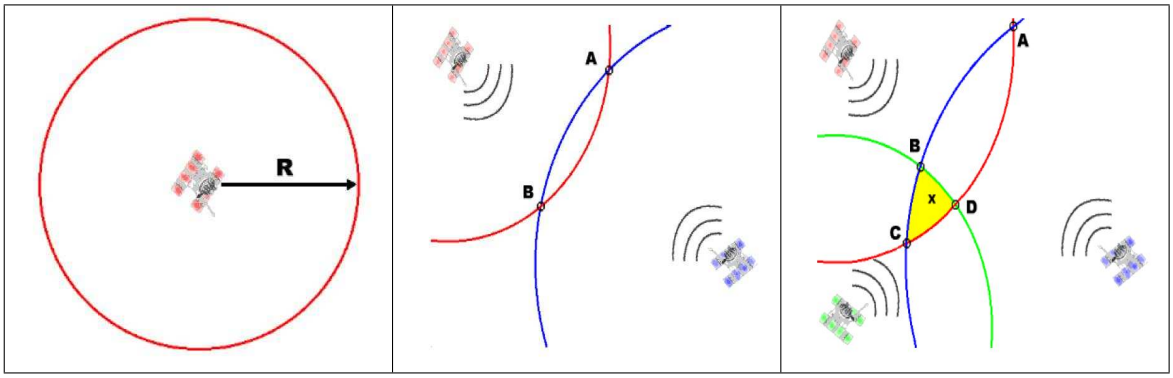

Figure 5: Pseudo range triangulation to get a position.

2.4.1. How accurate is GPS?

Today's GPS receivers are extremely accurate, thanks to their parallel multi-channel design. For example, a receiver with 12 parallel channels is today quick to lock up to 12 satellites simultaneously when turned on and it maintains strong locks, even in dense foliage or urban settings with tall buildings. Certain atmospheric factors and other sources of error can of course affect the accuracy of GPS receivers. The today's commercial GPS receivers are accurate to within 15 meters on average.

Newer GPS receivers with WAAS (Wide Area Augmentation System) capability can improve accuracy to less than three meters on average. No additional equipment or fees are required to take advantage of WAAS. Users can also get better accuracy with Differential GPS (DGPS), which involves the cooperation of two receivers, one that is stationary and another that is roving around making position measurements.

2.5. The GPS signals

GPS satellites transmit two low power radio signals, designated as L1 and L2. Civilian GPS uses the L1 frequency of 1575.42MHz in the UHF-band. At present time a modernization of the GPS is being implemented which will add a new civil signal called L5 which is at 1176.45MHz. The signals travel by line of sight, meaning they will pass through clouds, glass and plastic but will not go through most solid objects such as buildings and mountains. There are many factors that degrade the GPS signal and thus affect the accuracy. These are presented in a later chapter.

The GPS signal contains a Pseudo Random Noise code (PRN) with modulated Ephemeris and Almanac data, as well as satellite clock correction parameters, UTC translation parameters and ionospheric correction parameters.

Ephemeris data is transmitted within the NAV message and includes a very precise orbital and clock correction for a satellite. This data is necessary for a precise positioning. The Ephemeris data also contain important information such as status of the satellite (healthy or unhealthy), current GPS date, etc. Each satellite broadcasts only its own Ephemeris data and the data is only considered valid for about 30 minutes. Without this part of the NAV message, a GPS receiver would have no idea what the current time is and therefore is this part of the signal essential for determining a precise position.

Almanac data contains a reduced precision subset of satellite Ephemeris information for all satellites in the constellation. Almanac data allows the receiver to determine the location of any satellite at any time throughout the day, resulting in reduced acquisition time. Almanac data is not very precise and is considered valid for up to several months.

3. Simulation Overview

Figure 6 shows all the main blocks of functions that have been build to solve the task of this thesis. The pseudo range is the main output but all other sub-product variables are stored for later verification purposes and may be used for other utilizations. An interpretation of the simulation is given on next page, section 3.1.

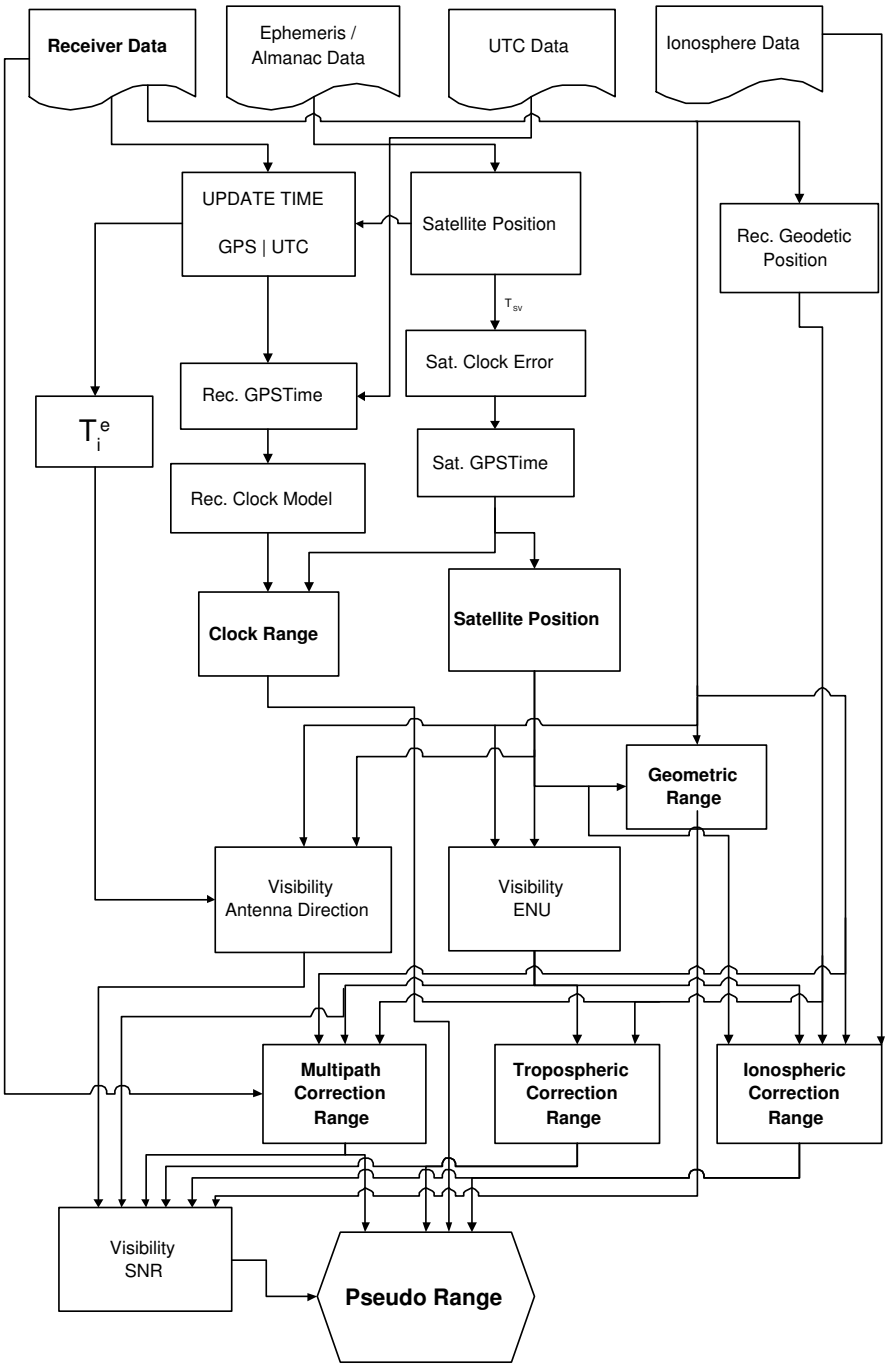

Figure 6: Simulation Program Schematic

3.1. Simulation Parts

As one can see in figure 6 the simulation is based on data from the NAV-message (Ephemeris/Almanac, UTC and Ionospheric data) and information from the receiver. All parameters in the receiver information must be stated by the user, or from a coupled program. Examples of receiver parameters are: Quaternions for the body frame (attitude parameters), the Body-Antenna transformation matrix, antenna mask, the receivers position in ECEF, date and UTC time. Note that the use of constants are not shown in the figure 6. Some of these can be found in appendix A.

Below are short descriptions of the main functions in the simulation (see figure 6):

Update Time: Update UTC time and conversion to GPS time.

Satellite position: Calculate the satellite position (ECEF).

Receiver Geodetic Position: Calculate the receiver's geodetic position (see appendix B.2.2).

Satellite Clock Error: Calculate the satellite clock correction to GPS system time at time of transmission. Calculate the satellite clock range error.

T_i^e**:** Calculation of the transformation matrix between ECI and ECEF reference frame.

Receiver Clock Model: Estimate the receiver clock bias and drift. Calculate the receiver clock range error.

Clock Range: Calculate the total clock range error.

Geometric Range: Calculate the geometric range between satellite and receiver. Calculate the range correction due to Earth rotation.

Visibility Antenna Direction: Calculate the satellite visibility due to the receiver antenna direction.

Visibility ENU: Calculate the satellite visibility due to Earth shadow etc.

Multipath Correction Range: Calculate the range correction due to multipath.

Tropospheric Correction Range: Calculate the range correction due to the tropospheric delay.

Ionospheric Correction Range: Calculate the range correction due to the ionospheric delay.

Visibility SNR: Calculate the signal to noise ratio.

Pseudo Range: Calculate the pseudo range between satellite and receiver.

4. Satellite Position

To calculate a GPS satellite position it is most suited to use the transmitted Almanac or Ephemeris data which are included in the NAV-message. The transmitted parameters values are such that they provide the best trajectory fit in Earth-centered, Earth-fixed Reference Frame coordinates (ECEF, see appendix B.2.1) for each specific fit interval. The orbital simulation is based on Kepler's laws and therefore, before it transforms the position into the ECEF, it describes the orbit of a satellite in orbital (Keplerian) elements. The elements/parameters that are required to get a functional simulation of the satellite position are:

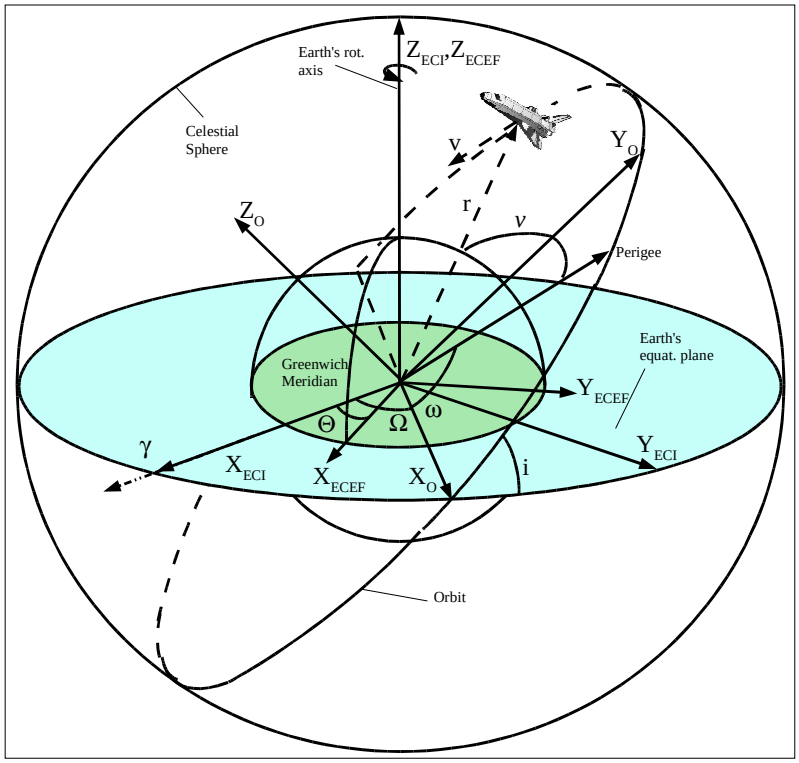

Figure 7: Orbital elements - 3D view.

- Ω_0 - right ascension of ascending node (rad)
- i - orbital plane inclination (rad)
- ω - argument of perigee (rad)
- a - semimajor axis of the spacecraft orbital ellipse (m)
- e - eccentricity of the spacecraft orbital ellipse (dimensionless)
- M_0 - Mean anomaly at reference time (rad)

4.1. Satellite Position Calculation

As discussed, the calculation of the satellite position is based on the Kepler's laws and therefore uses the Keplerian anomalies. These anomalies are defined:

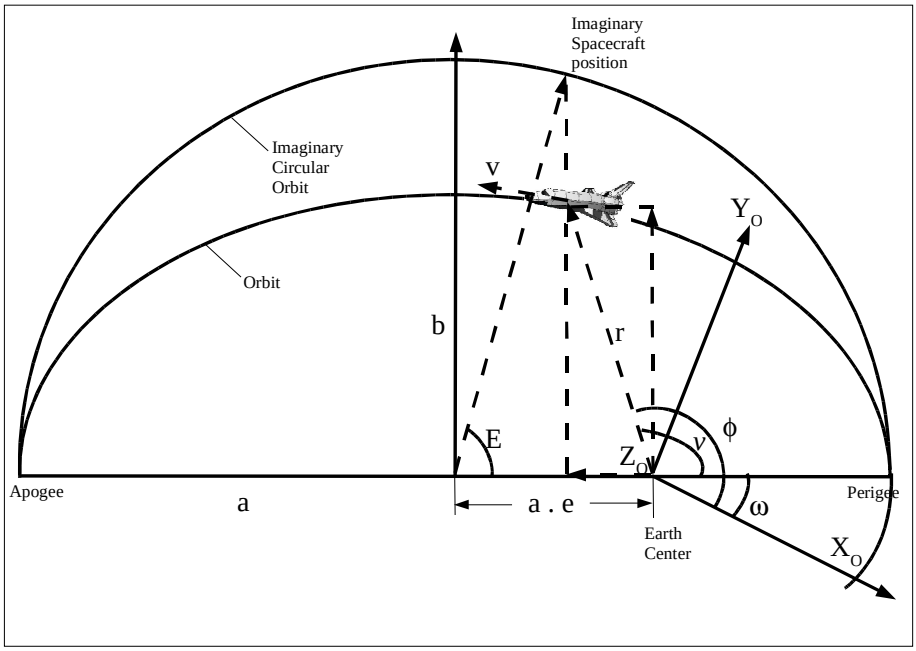

Figure 8: Orbital elements - 2D view.

- $v(t)$ - true anomaly - angle between the orbital perigee and the spacecraft current orbital position.
- $E(t)$ - eccentric anomaly - the angle measured at the center of the ellipse from pericenter to the point on the circumscribing auxiliary circle from which a perpendicular to the major axis would intersect the orbiting body.
- $M(t)$ - mean anomaly - mathematical abstraction.

From these anomalies the satellite position and velocity vector can be calculated in the orbital system plane. To perform the calculation with Ephemeris data following parameters are needed:

Var.	**Description**	**Unit**
T_0	Data reference time (referenced to GPS time)	s
Ω_0	right ascension of ascending node at reference time	$semi-circle$
i_0	orbit inclination at reference time	$semi-circle$
ω	argument of perigee	$semi-circle$
a	orbit semimajor axis	m
e	orbit eccentricity	-
M_0	mean anomaly at reference time	$semi-circle$

Table 1: Ephemeris Orbital Elements Data.

Note that one *semi-circle* is Π (pi) radians.

For the GPS time, t, the three anomalies are mathematically defined as ([13]):

$$M(t) = M_0 + n \cdot (t - T_0) \tag{1}$$

$$E(t) = M(t) + e \cdot sin(E(t)) \tag{2}$$

$$\nu_c = cos\left(\frac{cos(E(t)) - e}{1 - e \cdot cos(E(t))}\right), \quad \nu_s = sin\left(\frac{\sqrt{1 - e^2} \cdot sin(E(t))}{1 - e \cdot cos(E(t))}\right)$$
$$\nu(t) = atan(\frac{\nu_s}{\nu_c}) \tag{3}$$

The mean angular velocity, n, known as mean motion is given by Kepler's 3^{rd} law:

$$n_0 = \sqrt{\frac{\mu}{a^3}} \tag{4}$$

where μ is the massive body gravitational constant.
With the GPS Ephemeris correction (Δn) the mean motion is:

$$n = n_0 + \Delta n \tag{5}$$

The transcendental equation 2 is known as the Kepler's equation, which can be solved with a numeric method like Newton-Raphson ([13]):

$$E_{m+1} = E_m - \frac{E_m - e \cdot sin(E_m) - M}{1 - e \cdot cos(E_m)}, \quad m = 1, ...p \tag{6}$$

$$E_0 = M + \frac{e \cdot sin(M)}{1 - sin(M + e) + sin(M)} \tag{7}$$

where p is a defined number of iterations.

The spacecraft angular position in the orbital system plane $X_0Y_0Z_0$ (known as argument of latitude) follows from Figure 8:

$$\phi(t) = \nu(t) + \omega \tag{8}$$

The purely elliptical Kepler orbit is precise only for a two-body problem where the mutual gravitational attraction is the only force involved. In the actual GPS satellite orbit, perturbations due to the Sun, Moon and non spheric Earth's gravitational harmonics must be taken into account. Because of this are orbital correction parameters included in the Ephemeris data, see table 2.

Var.	Description	Unit
$\dot{\Omega}$	Rate of the right ascension of ascending node	$semi-circle/s$
Δn	mean motion difference	$semi-circle/s$
di/dt	orbit inclination rate	$semi-circle/s$
C_{us}	constant sinus amplitude for orbital angular position correction	rad
C_{uc}	constant cosine amplitude for orbital angular position correction	rad
C_{rs}	constant sinus amplitude for orbital radius correction	m
C_{rc}	constant cosine amplitude for orbital radius correction	m
C_{is}	constant sinus amplitude for orbital plane inclination correction	rad
C_{ic}	constant cosine amplitude for orbital plane inclination correction	rad

Table 2: Ephemeris Orbit Correction Data.

Hence, the GPS satellite orbit is modelled as a modified elliptical orbit with correction terms, which account for the perturbations in the argument of latitude

$$\delta u = C_{uc} cos2\phi + C_{us} sin2\phi \tag{9}$$

in the orbit radius

$$\delta r = C_{rc} cos2\phi + C_{rs} sin2\phi \tag{10}$$

and in the orbit inclination

$$\delta i = C_{ic} cos2\phi + C_{is} sin2\phi \tag{11}$$

where the constants C are transmitted correction sinus and cosine amplitudes.

Then, the perturbed values are:

$$u = \phi + \delta u \tag{12}$$

$$i_k = i_0 + \frac{di}{dt} \cdot t + \delta i \tag{13}$$

$$r = a \cdot (1 - e \cdot cos(E)) + \delta r \tag{14}$$

Furthermore, considering the Earth turn rate ω_E and the ascending node right ascension rate, the corrected longitude of ascending node is given by:

$$\Omega = \Omega_0 + (\dot{\Omega} - \omega_E) \cdot t - \omega_E \cdot t_{oe} \tag{15}$$

The position and velocity vector in the orbital reference frame are ([9]):

$$\underline{r}^0 = r \cdot \begin{bmatrix} cos(u) \\ sin(u) \\ 0 \end{bmatrix} \tag{16}$$

$$\underline{\dot{r}}^o = \sqrt{\frac{\mu}{a(1-e^2)}} \cdot \begin{bmatrix} -sin(u) \\ cos(u) + e \\ 0 \end{bmatrix} \tag{17}$$

To get the satellite position in $ECEF$ a transformation between the orbital XYZ_0 and the XYZ_{ECEF} is needed and it can be obtained through an Euler 3-1-3 rotation (see Appendix C.2), with first rotation around Z_0 axis with $-\omega$, second rotation around the resulting X axis with $-i$ and third rotation around the resulting Z axis with $-(\Omega - \Theta(t))$ through the rotation matrix $\underline{\underline{T}}^e_o(\omega, i, \Omega, \Theta(t))$:

$$\underline{\underline{T}}^e_o = \underline{\underline{T}}_3(-(\Omega - \Theta(t)))\underline{\underline{T}}_1(-i)\underline{\underline{T}}_3(-\omega), \quad \underline{\underline{T}}^o_e = (\underline{\underline{T}}^e_o)^T \tag{18}$$

with $\Theta(t)$ as a function of the Earth's angular rate ω_E:

$$\Theta(t) = \omega_E \cdot t \tag{19}$$

where t is given in UTC.

Hence, the position and velocity vectors in ECEF and in orbital system are:

$$\underline{r}^e = \underline{\underline{T}}^e_o \cdot \underline{r}^o, \quad \underline{r}^o = \underline{\underline{T}}^o_e \cdot \underline{r}^e \tag{20}$$

$$\underline{\dot{r}}^e = \underline{\underline{T}}^e_o \cdot \underline{\dot{r}}^o, \quad \underline{\dot{r}}^o = \underline{\underline{T}}^o_e \cdot \underline{\dot{r}}^e \tag{21}$$

4.2. UTC and GPS Time

GPS Time is represented in GPS Weeks and GPS Seconds from the start of GPS epoch, which is defined coincident to the Universal Time Coordinated (UTC) at 00:00:00 of January 5/6th 1980. Although GPS time was defined coincident to UTC, there are no insertions of leap seconds as in UTC in order to correct the deviation of Earth's rotation. This is because such insertion would cause the signal track loops to fail in the moment of insertion. Besides that, there is also inherent a drift rate with respect to UTC. Therefore is the GPS system time different from UTC and will be always ahead of it by a defined number of leap seconds.

To calculate the correct GPS satellite position one need to use the *GPS Time* at the NAV-message transmission. This time is not transmitted in the NAV-message instead are the satellites internal clock time and corrections parameters. A normal receiver calculate the GPS Time by comparing the phase displacement of received message with a own code. In a simulation like this, the GPS Time must be calculated from the *UTC Time* through following steps:

1. Converting the receiver UTC Time to GPS Time
2. Calculate the satellite position with the receiver GPS Time
3. Calculate time of signal propagation: $\Delta t = \frac{Satellite\ position\ -\ Receiver\ position}{Speed\ of\ light}$
4. Get Satellite GPS Time by subtract the propagation time from the receiver GPS Time
5. Iterate from step 2 with the new GPS Time until the difference between Δt is small enough.

In the first step, to convert UTC to GPS Time, one need to first convert the UTC Time to *Sidereal time* and then back to GPS time. This can be done from the definition of the *Julian calendar*. Sidereal time has units equal to the period of the Earth's rotation with respect to the fixed stars (equatorial angle between Greenwich reference meridian and fixed stars reference point). The Julian calender is a continuous count of days and fractions, which began at 12:00:00 UT, January 1st, 4713 B.C. The calculation of the Julian date is commonly used by astronomer in order to avoid the complexity of the other calendars.

Note the definition of GPS Time is in weeks and seconds which means that the GPS Time that is used in position calculation must be inside one week. Correction of the GPS Time is presented in chapter 6.1 (GPS Time is there represented by the satellite internal clock time, t_{SV}).

5. Satellite Visibility

Earth can shadow many GPS satellites and the receiver antenna can point in different directions. To get the GPS satellite visibility it is therefore important to know the elevation angle between receiver to the Earth horizon, and antenna direction to satellite. It exist of course other influences on the visibility, for examples the signal to noise ratio.
Note that in this project the receiver position is known and therefore it is of more concern to always use correct reference frame. An example of this is that the satellite position and the receiver antenna can be in different reference frames and a transformation to a common frame is needed. Information about the transformation between different reference frames can be found in appendix B.

5.1. Receiver-Satellite Angles

The azimuth and elevation between the receiver position (or antenna direction) and the satellite are the most important in visibility calculations. To guarantee that all calculations of azimuth and elevation are done in same reference frame, the equation 22 can be used ([2]):

$$\underline{r}^B = \underline{\underline{T}}^B_A \cdot (\underline{r}^A - \underline{r}^A_B) \tag{22}$$

where $\underline{\underline{T}}^B_A$ is the transformation matrix between the two reference frames A and B and $\underline{r}^A_B$ is the origin of frame B with respect to frame A. For example can the reference frames A and B represent *ECEF* resp. *ENU*.

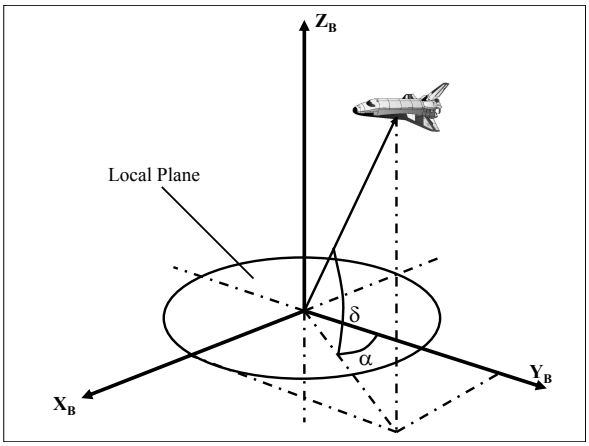

Figure 9: Azimuth and Elevation

The azimuth, α, and the elevation, δ, to a object in the reference frame B are given by following equations:

$$r^B_x = |\underline{r}^B| cos\delta sin\alpha, \quad r^B_y = |\underline{r}^B| cos\delta cos\alpha, \quad r^B_z = |\underline{r}^B| sin\delta \tag{23}$$

$$\alpha = atan2(r^B_x, r^B_y), \qquad \delta = asin\left(\frac{r^B_z}{|\underline{r}^B|}\right) \tag{24}$$

5.2. Satellite Visibility due to Earth Shadow

If the elevation between the receiver and satellite is over both the Earth horizon and the receivers elevation mask the satellite is geometrical visible for the receiver. To find out where the horizon of the Earth is relative to the receiver position, the following approximated calculation can be used since the Earth is an ellipsoid:

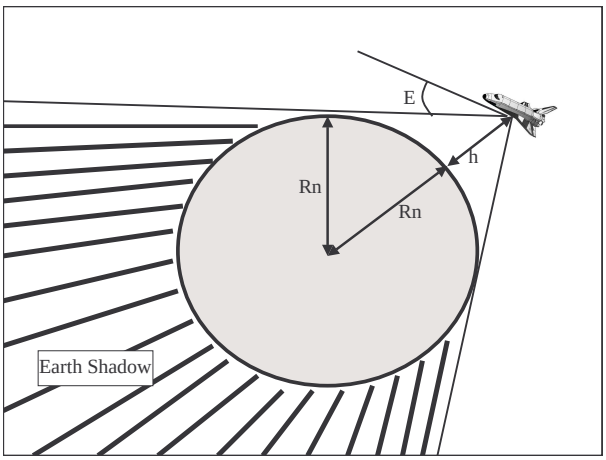

Figure 10: Earth can shadow out satellites

The elevation between a receiver and the horizon is approximated through following equation([6]):

$$Elevation_{sat}^{horizon} = acos\left(\frac{Rn}{Rn+h}\right) \tag{25}$$

where

$$Rn = \left(\frac{A_{Earth}}{\sqrt{1 - e_{Earth}^2 \cdot sin^2(lat)}}\right) \tag{26}$$

and Rn is the length of the normal from the ellipsoid surface to its intersection with Z-axes and the attitude of the receiver. h is the length from the same intersection point to the receiver. See figure 11.

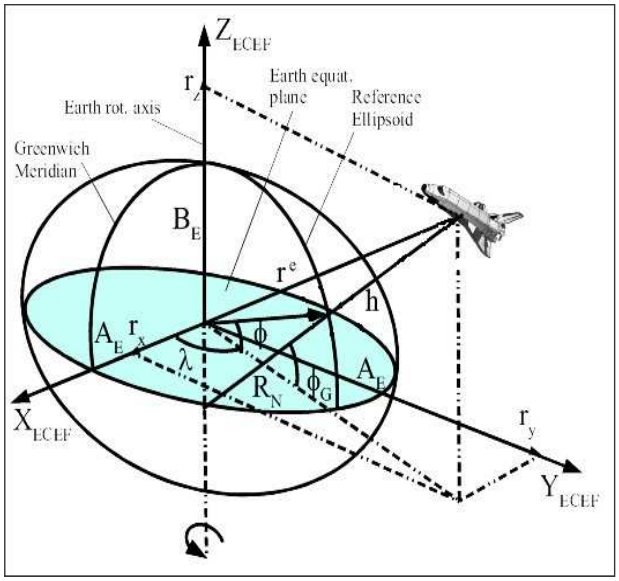

Figure 11: Visual view of Rn

Because Earth is an ellipsoid the 'radius' is calculated through Rn. This will give the radius an error, but for receivers near Earth the error will be relative small and for a receiver far from Earth's surface, this radius will act like if Earth was a sphere. The error act as a small elevation mask.

5.3. Satellite Visibility due to Receiver Position in Space

Navigation with help of using GPS in space is practical. This is of course only provided if one is inside the main beam of the GPS antenna and outside the Earth shadow. As figure 12 shows, the zenith angle of the main beam from transmitting GPS antenna relative to Earth is 21.3 degrees.

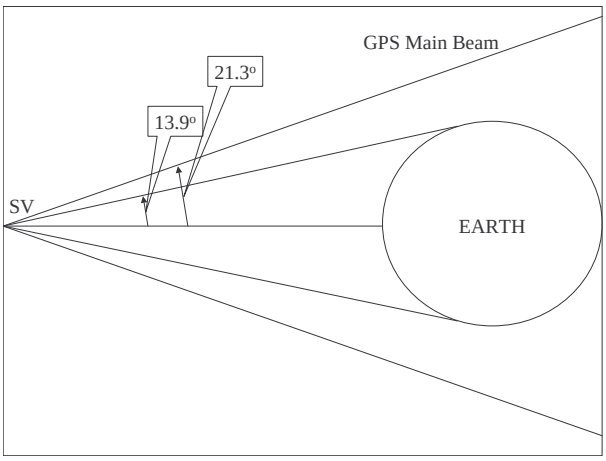

Figure 12: GPS Satellite transmitting antenna angles, [13].

If the receiver position and the GPS satellite position (both in ECEF) are known one can with help of the Sinus law calculate whether the receiver is inside the main beam or not. The receiver is inside if β in equation 27 is less than 21.3 degrees.

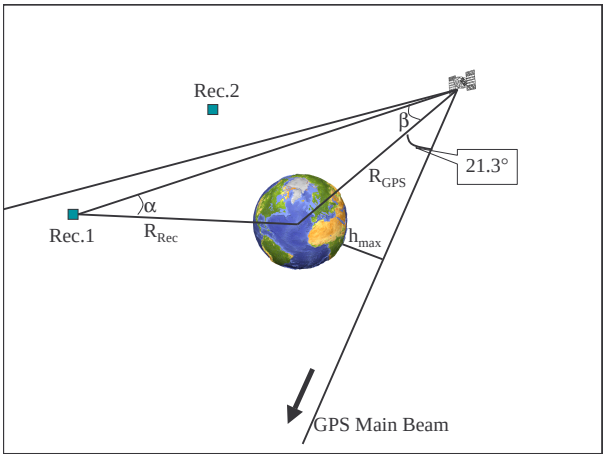

Figure 13: Satellite visibility due to receiver position in space and the GPS transmitting antenna beam.

$$\beta = \arcsin\left(\frac{r_{Rec} \cdot \sin\alpha}{r_{Sat}}\right) \tag{27}$$

As figure 13 shows is Rec.2 (Receiver 2) outside of the main beam and will therefore not receive any signal for given GPS satellite. Since the radius of the GPS satellites orbits are known a rough calculation gives that one need to be at least 3270km from the Earth surface (h_{max} in figure 13) to be outside the main beam of one GPS satellite.

5.4. Satellite Visibility due to Antenna

In the main simulator (in which this simulator will be used) the attitude of the body in the ECI reference frame is given as quaternions. Also the transformation matrix antenna to body (the position/direction of antenna on the body) and an antenna elevation mask are provided. With this information and knowledge of the satellite and receiver position the satellite visibility due to the antenna direction can be derived.

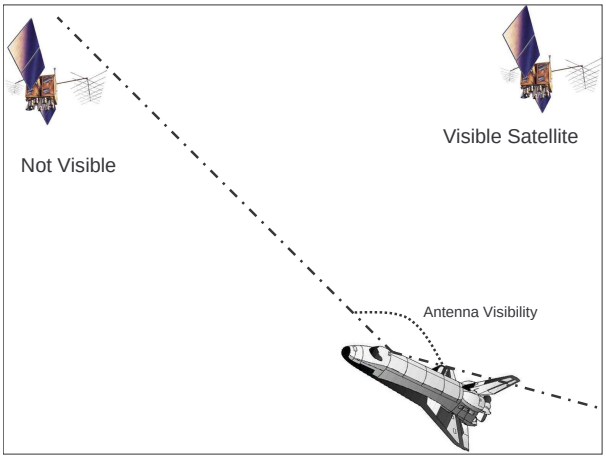

Figure 14: Different body and antenna attitudes can cancel out GPS signals

The quaternions represent the body attitude with respect to the ECI frame. For a mathematical overview of quaternions see appendix C.4. Following transformation matrix is used to obtain the corresponding rotation matrix from the given quaternions ([15]):

$$\underline{\underline{T}}_i^b(\underline{q}_i^b) = \begin{bmatrix} q_1^2 - q_2^2 - q_3^2 + q_4^2 & 2(q_1q_2 + q_3q_4) & 2(q_1q_3 - q_2q_4) \\ 2(q_1q_2 - q_3q_4) & -q_1^2 + q_2^2 - q_3^2 + q_4^2 & 2(q_2q_3 + q_1q_4) \\ 2(q_1q_3 + q_2q_4) & 2(q_2q_3 - q_1q_4) & -q_1^2 - q_2^2 + q_3^2 + q_4^2 \end{bmatrix} \tag{28}$$

To get the satellite angles (azimuth, elevation) with respect to the antenna the transformation matrix between $ECEF$ and the antenna must be applied. This transformation matrix is derived using the following equation:

$$\underline{\underline{T}}_e^a = \underline{\underline{T}}_b^a \cdot \underline{\underline{T}}_i^b \cdot \underline{\underline{T}}_e^i \tag{29}$$

Where $\underline{\underline{T}}_b^a$ is the given transformation matrix between the body and the antenna, $\underline{\underline{T}}_i^b$ is the transformation matrix presented in equation 29 above , ECI to body, and $\underline{\underline{T}}_e^i$ is the transposed $\underline{\underline{T}}_i^e$ matrix (ECI to $ECEF$) which is derived in B.3.

The visibility due to the antenna can be computed by comparing the elevation with respect to the antenna and a possible elevation mask.

5.5. Satellite Visibility due to Signal to Noise Ratio

The following information is compiled from [1], [4], [5], [10], [13].
GPS signals received on the Earth are extremely weak and therefore important when simulating the visibility of GPS satellites. The GPS signal is well below the background RF noise level sensed by an antenna. It is the knowledge of the signal structure (i.e. PRN code) that allows a receiver to extract the signal buried in the background noise and to make precise measurements. Table 3 gives a hint of what power levels one can expect to receive.

	L1 C/A Code
Minimum received power	-160.0 dBW
Maximum expected power	-152.0 dBW

Table 3: Received GPS signal power levels, [10].

These measurements are referenced to a power level of one Watt. However, absolute signal power is not necessarily meaningful, because it does not consider the power level of the background noise. Receiver performance is more dependent on a signal to noise power ratio than the absolute signal power.

In practice, the ratio of total carrier power to the noise density C/N_0 in dB-Hz is the most generic representation of signal power as it is independent of the implementation of the receiver front-end bandwidth and therefore gives a more generic signal strength characterization. But for a BPSK (Binary Phase Shift Keying) modulated waveform with a null-to-null bandwidth B_n, an approximation relationship of SNR and C/N_0 can be represented by equation 30:

$$SNR(dB) = \frac{S}{N} = \frac{C}{N_0}(dB - Hz) - B_n(dB) \tag{30}$$

where:

- C/N_0 - is a ratio of total carrier power to the noise power in one Hz of bandwidth
- B_n - Bandwidth of the filter in the receiver to remove out of band noise
- $\frac{S}{N}$ - is the signal to noise in B_n bandwidth

The equation for calculating the effective received C/N_0 is shown in equation 31.

$$\frac{C}{N_0} = EIRP + G_R + SL - kT - L - N_F(dB) \tag{31}$$

where:

- $EIRP$ - Equivalent Isotropic Radiated Power = transmitted power + transmitted antenna gain.
- G_R - Antenna gain toward the satellite

- SL - Free Space Loss = $\left(\frac{wave\ length}{4\pi \cdot distance}\right)^2$
- kT - Thermal noise density. Where k is Bolzmann's constant and T is the mean signal temperature of propagation.
- L - Atmosphere attenuation
- N_F - Receiver noise figure

The table 4 provides a range of power ratios, based on the combination of received power, ambient noise power, antenna gains and typical losses. The table does not account for signal attenuation by any unnatural interference. Note that the satellite power from Block II satellites often exceeds the specified level because the satellite power is expected to degrade with time, and newer satellites are designed to have a higher output than their end-of-life specification, perhaps by as much as 6dB. These differences in power levels are not accounted for here.

	Minimum received power and maximum receiver losses (dB)	**Maximum received power and minimum receiver losses (dB)**
Received signal power, C	-160	-152
Noise floor, N_0	-203	-205
C/N0	43	53
Noise figure, N_F	4	2
Receiver and Atmosphere Losses	2	1
Pre-Correlation, C/N0	37	50
Bandwidth, B_N	63.1	63.1
Pre-Correlation, S/N	-26.1	-13.1
Processing Gain, G_P*	33.1	33.1
Post-Correlation, S/N	7	17

Table 4: Received GPS signal levels (dB).

* The receivers processing gain (G_P) is defined as a ratio between the chipping period and the data bit period. Calculation of the processing gain is given by equation 32, ([4]):

$$\textbf{Processing Gain} = \frac{C/A\ code\ chipping\ rate \cdot 2}{Time\ to\ next\ repeat} = \frac{2 \cdot 1.023MHz}{\sim 1kHz} \tag{32}$$

The used reference receiver had a cutoff value at 10dB, which means that if the value is less then this the satellite signal level is to low for using in calculations. The table 4 represents the simulated signal to noise ratio and therefore has the simulation an cutoff value at 7dB.

5.5.1. Antenna Pattern

The GPS transmitted antenna pattern gain (G_T) is not equal over all elevations angels. This is shown below in figure 15 where gain at the zenith angle is zero decibel and at 13.9 degree is it -2.1dB, [13]. It is therefore important to consider the elevation when calculating the signal to noise ratio. And if the receiver does not have an omnidirectional antenna (receiver gain, $G_R = 0$dB), then the receiver antenna pattern plays a role.

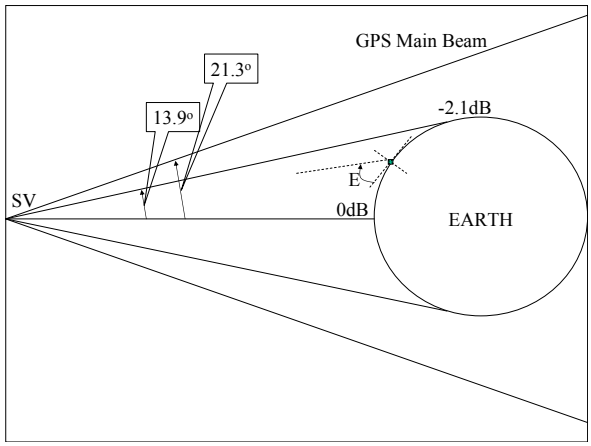

Figure 15: Atmospheric attenuation vs elevation in degrees.

Based on information from figure 15 above and the equation 33, an expression for the transmitted gain (G_T) due to the GPS antenna pattern is derived, equation 34.
When calculating the $EIRP$ in equation 31 the value from equation 33 is added to the total G_T (actual antenna gain + antenna pattern gain). Because the antenna pattern gain is never positive, the total transmitted gain will not be higher than the origin. The equation 33 is based on the graph of $y = \sin x$ and acts here as a simple approximation for the antenna pattern.

$$Gain(dB) = k \cdot \sin E + m \tag{33}$$

where E is the angle between the GPS satellite zenith angle and the receiver, in radians.

$$G_T(dB) = 2.5413 \cdot \sin E - 2.5413 \tag{34}$$

The used receiver antenna was an hemispheric receiver antenna with the following gain specifications: -3dB at 10° and 3.5dB at zenith. On the same way as for the GPS transmitted antenna gain an expression for the receiver antenna gain is derived, equation 35:

$$G_R(dB) = 7.8659 \cdot \sin E - 4.3659 \tag{35}$$

For the equation 35, E is the satellite elevation with respect to antenna. Figure 16 show how the transmitted response receiver antenna gain is due to the satellite elevation with respect to the receiver.

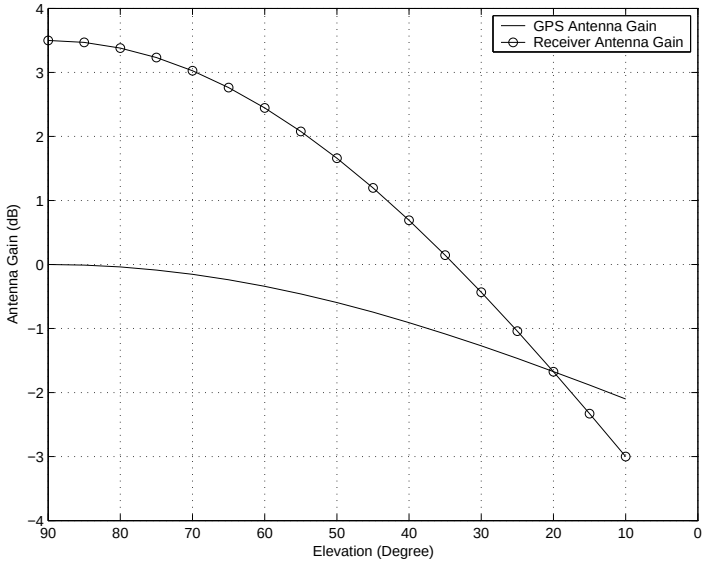

Figure 16: Transmitted degrade receiver response gain due to the elevation of the satellite.

5.5.2. Atmospheric Attenuation

Atmospheric attenuation in the 1-2GHz frequency band is dominated by oxygen attenuation. The attenuation varies with elevation angle E in proportion to the tropospheric path length L (mapping function). If the atmosphere is modelled by a simple uniform spherical shell with the height h_m above Earth then (see figure 17) the length of the path L varies with elevation angle E.

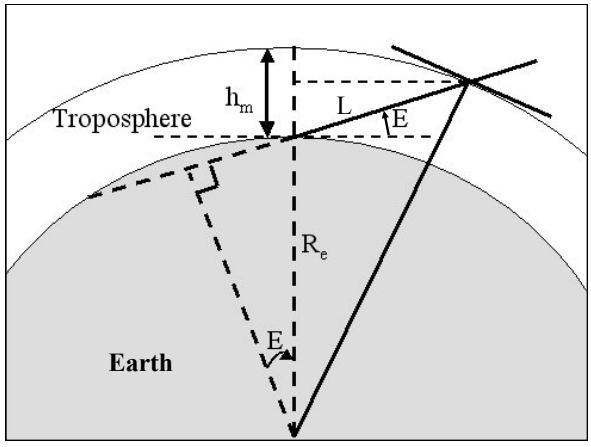

Figure 17: Path length L through a uniform shell troposphere at elevation E

Thus, the atmospheric attenuation, $A(E)$, has the following approximate value ([13]):

$$A(E) \cong \frac{2A(90^\circ)(1 + a/2)}{\sin E + \sqrt{\sin^2 E + 2a + a^2}} \tag{36}$$

where a $= h_m/R_e << 1$ and h_m is the equivalent height for oxygen, 6 km.

The attenuation of Equation 36 is shown in Fig 18. Note that this model is not accurate for elevation angles $E < 3°$, but since there are many error sources in this region an elevation mask of 5° often is applied and therefore are very low angles not important. The expression for $A(E)$ has assumed a spherical troposphere symmetrical in azimuth and with uniform density.

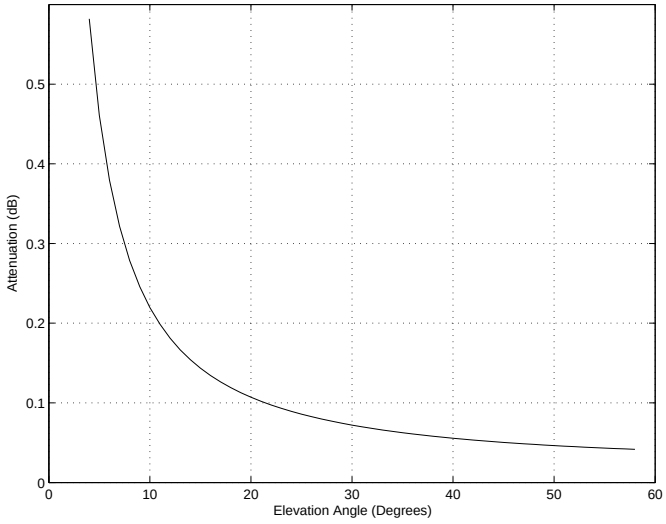

Figure 18: Atmospheric attenuation vs elevation in degrees.

Because the atmospheric attenuation has so little effect in the total signal link budget, the maximum attenuation, 0.6dB, will be chosen for all link budget calculations.

6. Pseudo Range

The pseudo range is a distance based on the satellite transmitted and the local receiver's reference code, that has not been corrected for errors in synchronization between the transmitter's clock and the receiver's clock. The term *pseudo range* is used because the time at the observer is only an estimate. In this project the receiver position is known and the satellite position is simulated from given data. It might be easy to just use the distance value between these two to get the pseudo range, by following equation:

$$R_{geometric} = \sqrt{(R_{Satellite} - R_{Receiver})^2} \tag{37}$$

But equation 37 only gives the geometric distance, or almost the geometric distance. To get the geometric distance one also need to correct for the Earth rotation at the time of received signal(see equation 38). The correction equation (eq. 39) of the Earth rotation is derived from the satellite position, receiver position and Earth rotation.

$$R_{geometric} = \sqrt{(R_{Satellite} - R_{Receiver})^2} + EarthRotCorr \tag{38}$$

where the Earth rotation correction is:

$$EarthRotCorr = \frac{\omega_E}{c}(x_{sat}y_{rec} - y_{sat}x_{rec}) \tag{39}$$

ω_E and c are the Earth turn rate and speed of light respectively (see appendix A). For stationary GPS receiver on Earth the rotation correction is about ± 20 meters.

Since the interest is to know the pseudo range one needs to include errors that affect the signal/code between the satellite and the receiver, and therefore: $R_{geometric} \neq R_{pseudorange}$. For a receiver the pseudo range contains a number of errors. Some of these errors can be estimated and used for corrections. A distinction must first be made between the errors that affect position accuracy, and those that affect GPS signal tracking. For example, errors that are slowly changing over time do not adversely affect the tracking performance of a GPS receiver, but they do affect the calculated position accuracy. An exploration of the main sources of errors in GPS is needed, but in this thesis are only those errors that one are able to model and important enough when comparing with a receiver design in focus. Following error/correction is included in the simulator:

- GPS Satellite clock error
- Receiver clock bias error
- Ionospheric delay
- Tropospheric delay
- Multipath range error

As stated by [13], there are transmitted data errors (error in the Ephemeris) and receiver error, such as noises and software accuracy, but these are not included in the

simulation.

With the discussed errors, the equation for calculating the pseudo range is:

$$R_{pseudo} = R_{Geometric} + c(\Delta T_{Rec} - \Delta T_{SV} + \Delta T_{Ion} + \Delta T_{Trop}) + \Delta R_{Multipath} \quad (40)$$

The largest part is represented by the true geometric range, $R_{Geometric}$. $\Delta R_{Multipath}$ is error due to the multipath. The delays, which are scaled by the speed of light to obtain a distance, are:

- ΔT_{Rec} - The receiver clock bias error time delay
- ΔT_{SV} - The Satellite clock bias error time delay
- ΔT_{Ion} - Ionospheric delay time delay
- ΔT_{Trop} - Tropospheric delay time delay

6.1. GPS Satellite Clock Error

Fundamental to the GPS is the one-way ranging that ultimately depends on satellite clock predictability. But error occurs in both the GPS satellite clock and receiver clock associated biases, drifts and if the message does not transmit the correct clock correction terms.

Different from GPS system time, the SV Time is the time maintained by each satellite. Every GPS satellite has four atomic clocks in a redundant system (two cesium and two rubidium). These atomic clocks have a approximal stability of about 1 part in 10^{13} over a day. If a clock can be predicted to this accuracy, its error in one day ($\sim 10^5$s) will be about 10^{-8}s or 3.5m, ([13]). Although each GPS satellite has precise internal clocks, it is not possible to keep them all closely synchronized to each other. Some degree of relative drift is allowed while they are monitored by the GPS control segment and occasionally reset to maintain time to within one-millisecond of GPS time. Furthermore, the signals are affected by other effects like Earth's rotation, relativistic drift and ionosphere delays. In order to correct such effects, the control segment frequently estimates such deviations and uploads correction terms to the satellite as clock correction data towards GPS time. These terms are then included by the satellite in the NAV message to be transmitted to the user. This corrections allow the user to compute the pseudo range in true GPS time, which is common for all satellites.

6.1.1. Satellite Clock and GPS Time Corrections

For correct use of the broadcasted Ephemeris/Almanac data for computing the satellite position, the transmission time related to GPS system time must be used. The satellite internal time t_{SV}, to which the transmission time is referenced originally, should not be used once the receiver clock is GPS time synchronized. While all data in TLM (telemetry word) and HOW (Hand-Over Word) are referred to the satellite internal time, data for NAV message are related to GPS system time.

Hence by means of the satellite internal time and GPS time corrections, the received code phase time with respect to the code offset and relativistic effects is corrected to permit the single frequency users (L1 or L2) to compensate group delay effects and to permit double frequency users (L1 and L2) to correct group propagation delay due to ionospheric effects.

Var.	**Description**	**Unit**
T_{GD}	group delay due to ionosphere *	s
t_{oc}	satellite clock reference time **	s
a_{f0}	satellite clock offset **	s
a_{f1}	satellite clock drift **	s/s
a_{f2}	satellite clock frequency drift **	s/s^2

Table 5: Satellite internal time correction data.
* Referenced to GPS time, ** Referenced to satellite internal clock

To resolve the transmission time in GPS system time, t_{GPS}, the satellite internal time t_{SV} must first be determined. To determine it, the receiver take use of the received GPS signals, its internal clock and approximate satellite pseudo range estimations. How this is done is presented in chapter 4.2.
The GPS time is then obtained by:

$$t_{GPS} = t_{SV} - \Delta t_{SV} \ (s) \tag{41}$$

where the offset correction is

$$\Delta t_{SV} = a_{f0} + a_{f1}(t_{GPS} - t_{oc}) + a_{f2}(t_{GPS} - t_{oc})^2 + \Delta t_r \tag{42}$$

where Δt_r is the relativistic correction and is needed due to time dilatation between satellite and user.

Note that the equations 41 and 42 are coupled. However, it is possible to use $t_{GPS} = t_{SV}$ in equation 42 (see [8]), accounting that in this case the t_{GPS} is at most 1/2 week distant from the satellite clock reference time t_{oc} ($1/2week = 302400s$, $1week = 604800s$):

$$t_{GPS} \Leftarrow \begin{cases} t_{GPS} - 604800, & t_{GPS} - t_{oc} > 302400 \\ t_{GPS} + 604800, & t_{GPS} - t_{oc} < -302400 \end{cases} \tag{43}$$

The relativistic correction, Δt_r, is:

$$\Delta t_r = F \cdot e \cdot \sqrt{a} \cdot sin(E_k), \quad F = -2\frac{\sqrt{\mu}}{c^2} = -4.442807633 \cdot 10^{-10} \ s/m^{1/2} \tag{44}$$

where the eccentric anomaly E_k is calculated from the Kepler's equation using the Newton-Raphson numeric method shown in [13]:

$$E_0 = M + \frac{e \cdot sin(M)}{1 - sin(M + e) + sin(M)} \tag{45}$$

$$E_{n+1} = En - \frac{E_n - e \cdot sin(E_n) - M}{1 - e \cdot cos(E_n)}, \quad n = 1, ...p \tag{46}$$

where p is a defined number of iterations and the mean anomaly is:

$$M = M_0 + n \cdot (t_{GPS} - t_{oe}), \quad n = \sqrt{\frac{\mu}{a^3}} + \Delta n \tag{47}$$

Since the used receiver in this project is a single frequency receiver, the correction Δt_{SV} calculated above must be corrected using T_{GD}, this because a_{f0} is defined for dual frequency users:

$$\Delta t_{SV_{L1}} = \Delta t_{SV} - T_{GD} \tag{48}$$

$\Delta t_{SV_{L1}}$ is the bias error and represent the ΔT_{SV} in the *Pseudo Range* equation (equation 40).

6.2. Receiver clock error

Since the receiver clock neither have an accurate atomic clock or its offset is known a simulation model is needed. Usually the total clock error is one of the four unknowns in calculation of the user position but since the receiver position already is known it is interesting for this simulation to model how the error of the receiver clock can act. The clock model that is presented in [13] (p.417) is used in this study.

In this model the clock bias and drift, which represent the phase and frequency errors, of the receivers crystal oscillator are estimated. Both the frequency and phase are expected as random walk. The discrete process equations are following:

$$x_c(k) = \Phi_c(\Delta t)x_c(k-1) + w_c(k-1) \tag{49}$$

where

$$x_c \equiv \begin{bmatrix} b \\ f \end{bmatrix}, \quad \Phi_c(\Delta t) = \begin{bmatrix} 1 & \Delta t \\ 0 & 1 \end{bmatrix}$$
$$Q_c \equiv E[w_c w_c^t] = \begin{bmatrix} S_b \Delta t + S_f \frac{\Delta t^3}{3} & S_f \frac{\Delta t^2}{2} \\ S_f \frac{\Delta t^2}{2} & S_f \Delta t \end{bmatrix}$$

b and f are the clock bias resp. clock frequency, Δt is the time between samples and the white noise spectral amplitudes S_b and S_f can be related to the classical Allan variance parameters. For temperature controlled crystal oscillators commonly used on commercial GPS receiver these are ([13]):

$$S_b = 4 \cdot 10^{-19} \qquad S_f = 16\pi^2 \cdot 10^{-20}$$

Since Matlab do not have the function of white noise a normalized Gaussian random function with the variance $\sigma^2 = 1$ is used instead.

ΔT_{Rec} in the *Pseudo Range* equation 40 is represented by:

$$\Delta T_{Rec} = b + \Delta t \cdot f \tag{50}$$

6.3. Ionospheric correction

The Ionosphere is a layer of the earth atmosphere extending from 50 km up to 1000 km above Earth. The ionosphere consists of gases that have been ionized by solar radiation. The ionization produce clouds of free electrons that act as a dispersive medium for GPS signals in which propagation velocity is delayed in proportional to the number of free electrons encountered and to the inverse of the carrier frequency squared ($1/f^2$). This means that it will be a time-of-arrival error at the receiver. The path delayed distance for a satellite at zenith is typically about 1m at night to 5-15m during late afternoon. At low elevation angles the propagation path through the ionosphere is much longer, so the corresponding delays can increase to several meters at night and as much as 50m during the day ([8]).

Since the ionosphere is a dispersive medium (the refraction index is a function of the operating frequency) it is easy for dual frequency receivers to compare the two frequencies and correct for the ionospheric error. But for civilian user with only one carrier signal (L1), the ionospheric effects must be considered in the time correction. This can be done by applying the **Klobuchar's** ionospheric model [11] which uses the transmitted ionospheric correction data in the NAV message. The control segment updates these parameters at least once each 6 days. The **Klobuchar's** ionospheric correction model is a simple model but provides at least 50% of reduction in the ionospheric delay. What **Klobuchar's** model actually do is to compute the amount of electrons (based on the angle to the magnetic pole) in one square meter at a intermediate point in the ionosphere and multiply it over the ionospheric distance. The formed tube is then related to a time delay.

The **Klobuchar's** ionospheric model is defined for users below the ionospheric top layer. Therefore must situations for a spaceborne receiver be treated separately, i.e. a receiver with an altitude over the ionosphere has still influence of the ionosphere since it can see satellites through it, see fig 19.

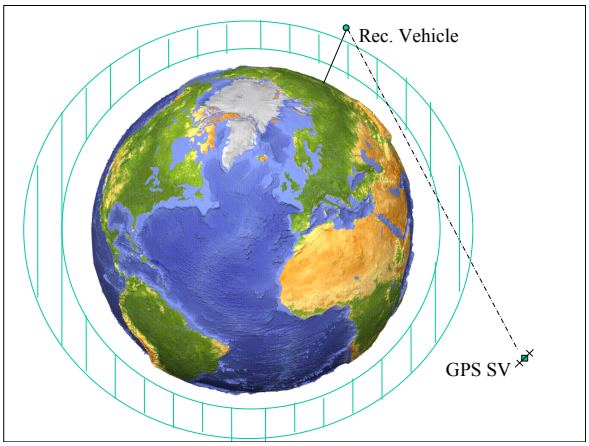

Figure 19: Ionospheric influence on signals when receiver is over the ionosphere

Ionospheric correction parameters provided by the satellite.

Var.	**Description**	**Unit**
α_0	vertical delay coefficient	s
α_1	vertical delay coefficient	$s/semi-circle$
α_2	vertical delay coefficient	$s/semi-circle^2$
α_3	vertical delay coefficient	$s/semi-circle^3$
β_0	period coefficient	s
β_1	period coefficient	$s/semi-circle$
β_2	period coefficient	$s/semi-circle^2$
β_3	period coefficient	$s/semi-circle^3$

Table 6: Ionospheric correction data parameters.

To use the correction data, a computed intermediated point, IP, of the path for the satellite signal to the user through the ionosphere is defined. The evaluation of the ionospheric model can be summarized as ([9], [3]):

- Compute the satellite zenith angle z with respect to the user:

$$z = \frac{\pi}{2} - elevation \tag{51}$$

- Define point IP:
  The point IP is defined by a vector calculated with basis on the rotation of the user unit vector about an axis perpendicular to the User-Earth Centered-Satellite plane to the point IP:

  Axis:

$$\underline{rp}^e = \underline{r}_S^e \times \underline{r}^e \tag{52}$$

  where $\underline{r}^e$ and $\underline{r}_S^e$ are the user and satellite ECEF positions.

  Angle:

$$\underline{\hat{e}}^e = \frac{\underline{rp}^e}{|\underline{rp}^e|} \tag{53}$$

  The distances to the top ionosphere layer about Earth's center can be approximated by:

$$ri_{max} = R_N + hi_{max} \tag{54}$$

$$ri_{min} = R_N + hi_{min} \tag{55}$$

  where $hi_{min} = 50\ km$ and $hi_{max} = 1000\ km$ are the assumed ionosphere low and top layer heights. R_N is the length of the user's normal from the ellipsoid surface to its intersection with Z_{ECEF} ([2]) and is defined as a function of Earth semi major axis A_E, Earth eccentricity e_E and the user geodetic latitude ϕ_G:

$$R_N = \frac{A_E}{\sqrt{1 - e_E^2 sin^2 \phi_G}} \tag{56}$$

Then, considering the computations all contained in the User-Earth Center-Satellite plane (see Figures 20 and 21):

$$\gamma = \frac{\pi}{2} + el \tag{57}$$

Through Sinus law:

$$\delta_1 = asin\left(|\underline{r}^e|\frac{sin(\gamma)}{ri_{max}}\right) \tag{58}$$

To determine the point IP there are 2 situations which must be considered:

1. The user is below the low ionosphere layer:

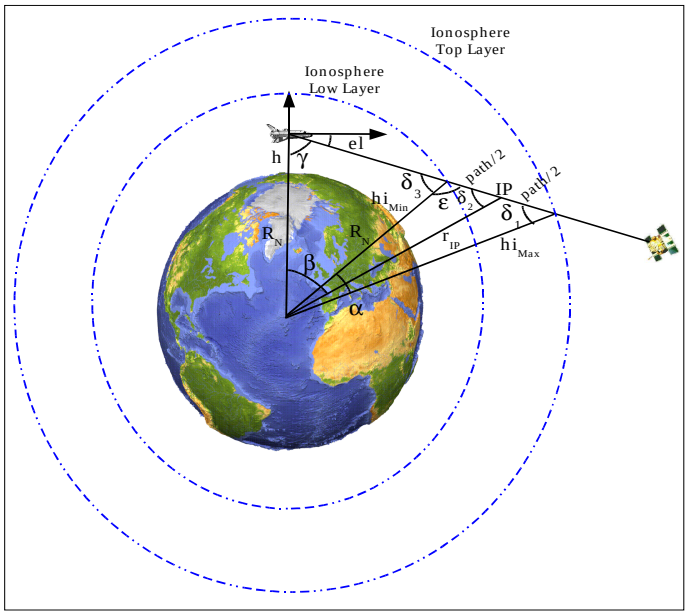

Figure 20: IP definition for heights below low ionospheric layer.

$$\delta_3 = asin\left(|\underline{r}^e|\frac{sin(\gamma)}{ri_{min}}\right) \tag{59}$$

$$\varepsilon = \pi - \delta_3 \tag{60}$$

Through Triangle's law:

$$\alpha = \pi - \delta 1 - \varepsilon \tag{61}$$

$$path = \frac{sin(\alpha)}{sin(\varepsilon)} ri_{max} \tag{62}$$

Through Median's law:

$$r_{IP} = \frac{1}{2}\sqrt{2(ri_{min}^2 + ri_{max}^2) - path^2} \tag{63}$$

2. The user is above the low ionosphere layer:

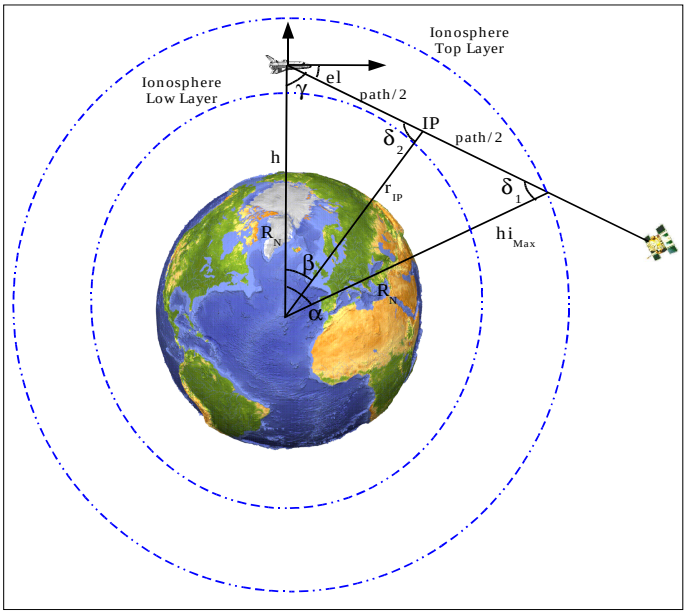

Figure 21: IP definition for heights above the low ionospheric layer.

$$\alpha = \pi - \delta 1 - \gamma \tag{64}$$

$$path = \frac{sin(\alpha)}{sin(\gamma)} ri_{max} \tag{65}$$

$$r_{IP} = \frac{1}{2}\sqrt{2(|\underline{r}^e|^2 + ri_{max}^2) - path^2} \tag{66}$$

and then after the height was treated, for both cases:

$$\delta_2 = asin\left(|\underline{r}^e|\frac{sin(\gamma)}{r_{IP}}\right) \tag{67}$$

$$\beta = \pi - \delta 2 - \gamma \tag{68}$$

IP Point:

$$\hat{\underline{r}}^e = \frac{\underline{r}^e}{|\underline{r}^e|} \tag{69}$$

$$\hat{\underline{r}}^e_{IP} = \underline{\underline{T}}(\hat{\underline{axis}}^e, -\beta)\hat{\underline{r}}^e \tag{70}$$

$$\underline{r}^e_{IP} = \hat{\underline{r}}^e_{IP} \cdot r_{IP} \tag{71}$$

where $\underline{\underline{T}}(\hat{\underline{e}}^e, -\beta)$ is a rotation matrix defined from the Euler rotation axis $\hat{\underline{e}}^e$ and angle $-\beta$ ([2]).

However, if $el = \pi/2$, to avoid singularities in the *path* calculation, r_{IP} can instead be approximated as:

$$r_{IP} = \begin{cases} R_N + (hi_{min} - h) + (hi_{max} - hi_{min})/2, & h \leq hi_{min} \\ R_N + h + (hi_{max} - h)/2, & h > hi_{min} \end{cases} \tag{72}$$

and:

$$\underline{r}^e_{IP} = \hat{\underline{r}}^e \cdot r_{IP} \tag{73}$$

Once $\underline{r}^e_{IP}$ is obtained, it is possible to calculate the latitude ϕ_{IP}, longitude λ_{IP} and height h_{IP} for the middle point IP (see [2]).

- Calculate the spherical distance from IP to the Earth's geomagnetic pole in semi-circles:

$$\begin{aligned} \theta^m_{IP} &= acos(sin(\phi_{IP})sin(\phi_P) + cos(\phi_{IP})cos(\phi_P)cos(\lambda_{IP} - \lambda_P)) \quad (rad) \\ \theta sc^m_{IP} &= \frac{\theta^m_{IP}}{\pi} \quad (semi - circle) \end{aligned} \tag{74}$$

where the geomagnetic pole coordinates $\phi_P = 78.3^o N$ and $\lambda_P = 291.0^o E$ have to be translated into radians.

- Calculate delay cosine period and amplitude from transmitted correction terms α_n, β_n, about IP:

$$AMP_{IP} = \begin{cases} \sum_{n=0}^{3} \alpha_n (\theta sc^m_{IP})^n, & AMP_{IP} \geq 0 \\ 0, & AMP_{IP} < 0 \end{cases} \quad (s) \tag{75}$$

$$PER_{IP} = \begin{cases} \sum_{n=0}^{3} \beta_n (\theta sc^m_{IP})^n, & PER_{IP} \geq 72000 \\ 72000, & PER_{IP} < 72000 \end{cases} \quad (s) \tag{76}$$

- Compute **Klobuchar's** zenith delay:
The correction term is treated as a half-cosine function. This function drops the ionosphere activity to a specified minimum during night periods while the maximum activity is a function of the local solar time.

$$T_{Iono-L1-Z} = \begin{cases} 5.0 \cdot 10^{-9} + AMP_{IP} \cdot cos(x_{IP}), & |x_{IP}| < \pi/2 \ \text{(day)} \\ 5.0 \cdot 10^{-9}, & |x_{IP}| \geq \pi/2 \ \text{(night)} \end{cases} \quad (s) \tag{77}$$

The delay phase due local time is:

$$x_{IP} = 2\pi \frac{t_{IP} - t_{14}}{PER_{IP}} \quad (rad) \tag{78}$$

where $t_{14} = 50400\ s$ is number of seconds at 14 h local time and IP local time is:

$$t_{IP} = t_{UTC} + \lambda_{IP} \cdot \frac{180}{\pi} \cdot \frac{3600}{15} \quad (s) \tag{79}$$

- Apply delay obliquity factor:

$$T_{Iono-L1} = F \cdot T_{Iono-L1-Z} \tag{80}$$

where the obliquity factor is defined as:

$$F = \frac{1}{cos(z')} \tag{81}$$

and z' is the satellite zenith angle at IP given by

$$z' = asin\left(\frac{R_N}{R_N + h_{IP}} sin(z)\right) \tag{82}$$

To use the shown equations, the user must be defined inside the ionosphere, in order for the expressions to be valid. However a problem arises when the user is outside the ionosphere but still receives signals whose elevation angle has a value below of that defined for the layers el_I, then passing through it.

$$el_I = -arccos\left(\frac{R_N + h_I}{R_N + h}\right) \tag{83}$$

where h_I shall be replaced by hi_{min} or hi_{max}.

The effect in this case can be computed in a similar way as done before, but using an effect calculation point ECP and its related elevation el_{ECP} as basis, which is defined in the near user intersection of the path with the ionosphere layer in question (See Figure 22). From this point on, everything is computed as the user were in this point.

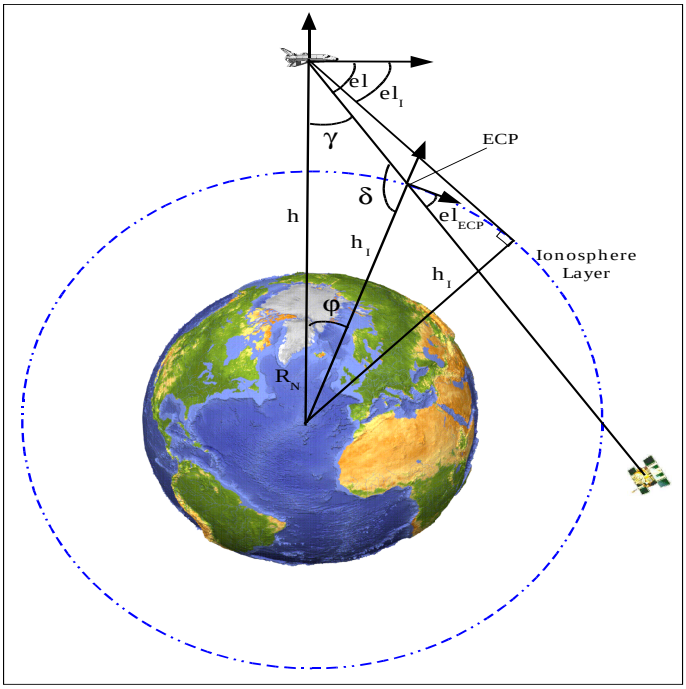

Figure 22: Ionospheric path delay for users outside the ionosphere.

If $el \leq el_I$, the ECP point is defined by a vector calculated with basis on the rotation of the user unit vector about an axis perpendicular to the User-Earth Center-Satellite plane to the near user intersection point:

The axis is calculated the same way as by Equations 52 and 53.

Angle:

$$\gamma = \frac{\pi}{2} + el \tag{84}$$

$$r_I = R_N + h_I; \tag{85}$$

$$\delta = \pi - asin\left(|\underline{r}^e|\frac{sin(\gamma)}{r_I}\right) \tag{86}$$

where π was included to guarantee that $\delta > \pi/2$.

$$\varphi = \pi - \gamma - \delta \tag{87}$$

ECP Point:

$$el_{ECP} = \pi/2 - \delta \tag{88}$$

$$\hat{\underline{r}}^e = \frac{\underline{r}^e}{|\underline{r}^e|} \tag{89}$$

$$\hat{\underline{r}}^e_{ECP} = \underline{\underline{T}}(\hat{\underline{e}}^e, -\varphi)\hat{\underline{r}}^e \tag{90}$$

$$\underline{r}^e_{ECP} = \hat{\underline{r}}^e_{ECP} \cdot r_I \tag{91}$$

Once $\underline{r}^e_{ECP}$ is obtained, it is possible to calculate the latitude ϕ_{ECP}, longitude λ_{ECP} and height h_{ECP} for the effect calculation point ECP (see [2]).

All the considerations shown above must be taken for both ionosphere layers with their respective heights. It is worth to say that this process must be taken twice in the case that the elevation results on the crossing of both layers. Thus, if $h > hi_{max}$, $el \leq el_{Imax}$ and $el \leq el_{Imin}$ an ECP must be calculated first for the top layer and then using the resulting point, a new ECP must be calculated for the low layer.

At this point it is worth to say that, although all computations involving IP have approximations in order to ease the process, it is only in the geometrical sense and does not change the original **Klobuchar's** model. Since its accuracy can reach at most 50% when calculated on the ground ([13]), considering the height helps to keep the model valid and avoids worse calculation results.
In the case of the ECP, it is a trial on considering some ionospheric delay in low elevation signals when their use can not be avoided (GPS outages for example). Although there are also geometrical approximations involved, it is anyway better to consider some delay in the signal than not considering any effect at all. However since negative elevation sights would be ignored by setting elevation masks above horizon under normal conditions, this computation would not take place most of time.

The following figures show the ionospheric path delay effect examples for different situations at user geodetic angles $\phi_G = 0^o$ and $\lambda_G = 0^o$ (Remember that the ionospheric effect is in function of the spherical distance of IP with respect to Earth's geomagnetic pole θ^m_{IP}.

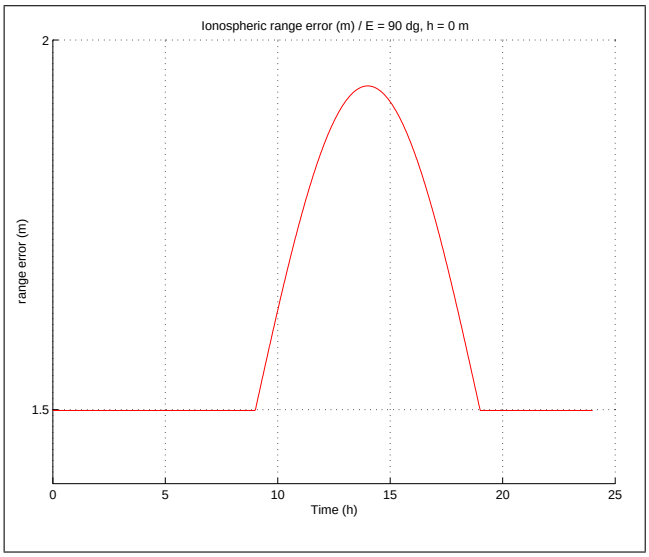

Figure 23: Ionospheric daily path delay model. User at (lat=0, lon=0).

The figure above shows the previously presented **Klobuchar's** model for the ionospheric daily effect, which is obtained by means of setting a imaginary static satellite at zenith with respect to the user and changing the local solar time.

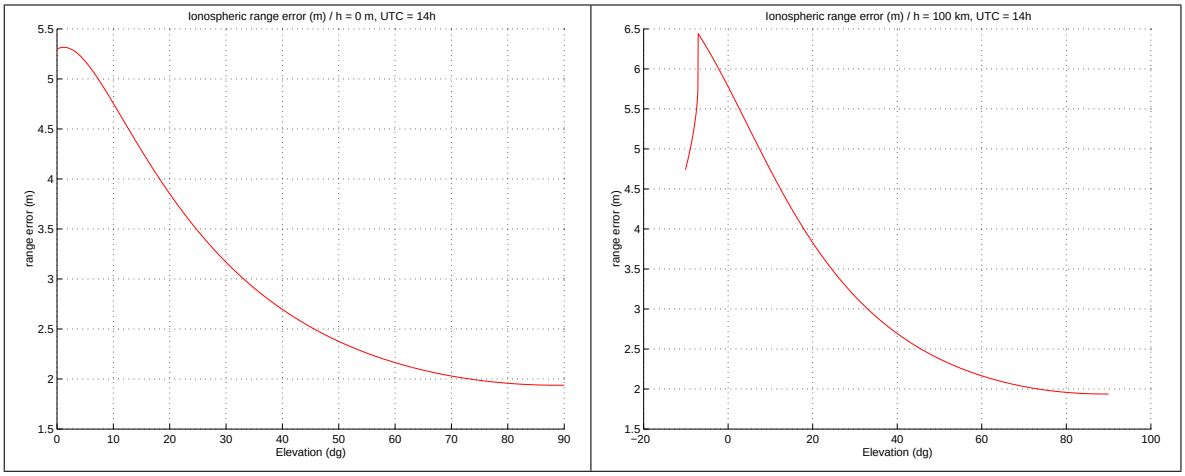

Figure 24: Ionospheric path delay for different elevations. dg=degrees. User at (lat=0, lon=0).

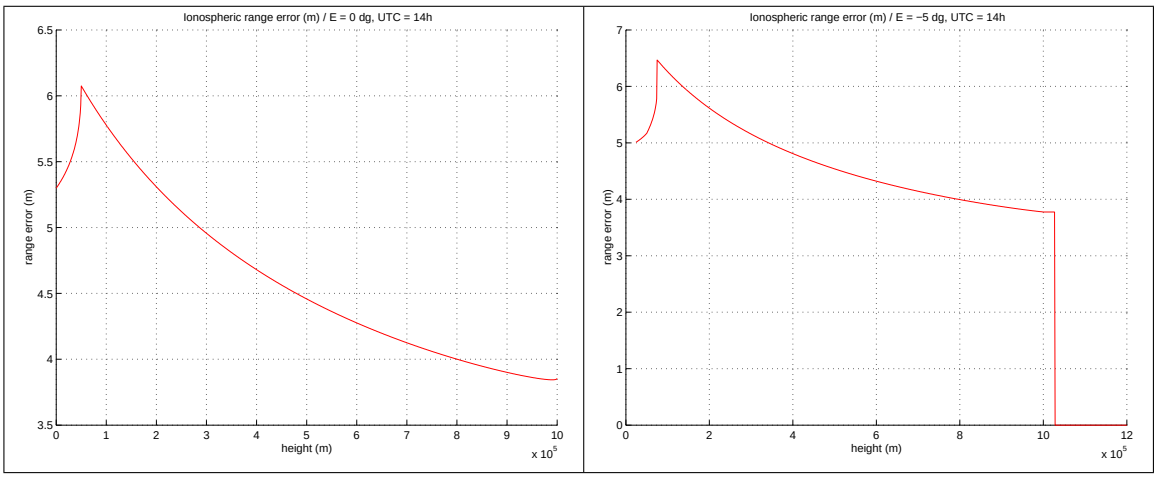

Figure 25: Ionospheric path delay for different heights. User at (lat=0, lon=0).

6.4. Tropospheric correction

Similar to the ionosphere, the troposphere also affects the propagation speed of the GPS signal. The Troposphere is the lower part of the atmosphere and is a non dispersive medium with respect to RF up to 15GHz. Thus, for GPS signals, the tropospheric delay is frequency independent, which means that there is no distinction for the delay for carriers L1 and L2. This makes the dual frequency elimination method, as can be used for ionosphere, impossible. There are three main effects: refraction, attenuation and scintillation, but of these it is usually only refraction caused by the wet and dry atmosphere that produce excess delay in the signal. The dry component is stable and predictable while the wet varies greatly. Therefore does variation in temperature, pressure, and humidity all contribute to variation in the propagation speed for radio waves.

Regarding the dry part of atmosphere and the water vapor, the GPS signal delay due to the troposphere can be considered by the **Hopfield's** model for the two different components, dry and wet ([9]):

$$T_{Tropo} = T_{Tropo-Dry} + T_{Tropo-Wet} \quad (s) \tag{92}$$

The **Hopfield's** model is based on the path distance that the signal have through the troposphere. Since both pressure and temperature changes with altitude can each component in the **Hopfield's** model be described as:

$$T_{Tropo-Dry}(h, el) = \frac{1}{c}\frac{10^{-6}}{5} N_{dry,0} \frac{(h_{dry} - h)^5}{h_{dry}^4}\, m_{dry}(el) \quad (s)$$

$$T_{Tropo-Wet}(h, el) = \frac{1}{c}\frac{10^{-6}}{5} N_{wet,0} \frac{(h_{wet} - h)^5}{h_{wet}^4}\, m_{wet}(el) \quad (s) \tag{93}$$

where the tropospheric dry and wet layer heights are:

$$\begin{aligned} h_{dry} &= [40136 + 148.72(T_0 - 273.16)] \ \ (m) \\ h_{wet} &= 11000 \ \ (m) \end{aligned} \tag{94}$$

the dry and wet refractivities at sea level are:

$$\begin{aligned} N_{dry,0} &= 77.64\frac{p_0}{T_0} \\ N_{wet,0} &= (-12.96T_0 + 3.718 \cdot 10^5) \cdot \frac{e_0}{T_0^2} \end{aligned} \tag{95}$$

the elevation mapping functions are:

$$\begin{aligned} m_{dry}(el) &= \frac{1}{\sqrt{el^2 + 6.25}} \\ m_{wet}(el) &= \frac{1}{\sqrt{el^2 + 2.25}} \end{aligned} \tag{96}$$

and h (m) is the user height, el $(degree)$ is the satellite elevation with respect to the user. The adopted standard atmosphere is:

- $p_0 = 10.13$ mb - atmospheric pressure
- $T_0 = 288.16$ K - temperature
- $e_0 = 0.085$ mb - partial pressure of water (50% humidity adopted)

To use the shown equations, the user position must be analyzed, in order to prove that the expressions are still valid. As the height grows, the sight to the satellite can acquire negative elevations, which can invalidate the elevation mapping function. Another problem also arises when the user is outside the dry and/or wet troposphere but still receives signals from satellites passing through them. Thus, there are 3 situations that must be considered by a navigating algorithm considering both dry and wet troposphere top layers:

1. User inside dry/wet troposphere + positive elevation

In this case the computation is easily done by using the standard equations shown above. No special treatment is required.

2. User inside dry/wet troposphere + negative elevation

In this case the elevation mapping functions would be invalid. It is possible to avoid this difficulty by computing a intermediary point IP in the signal path which line is orthogonal to Earth center. Then the effect is computed as a function of the effect which would be sensed in this point having the satellite at $el = 0$. (See Figure 26).

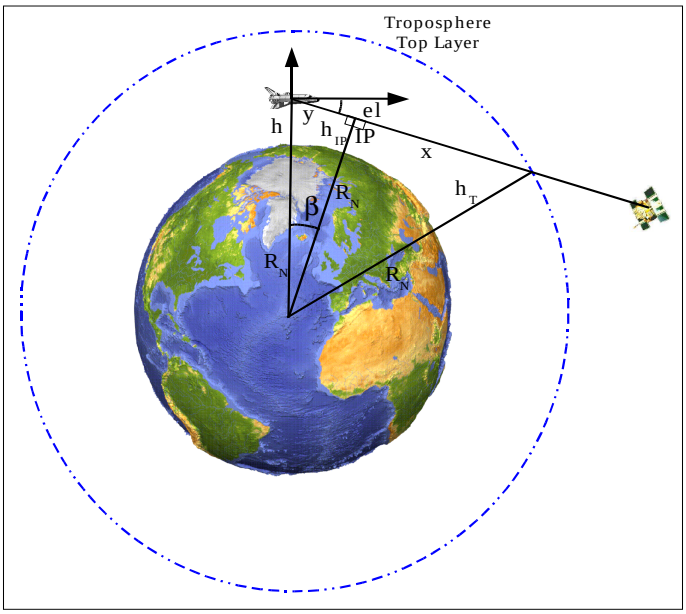

Figure 26: Tropospheric path delay for negative elevations inside troposphere.

By observing the figure it is possible to realize that the angle β is equal to the satellite elevation angle viewed from observer ($\beta = el$). Also by observing the figure the IP height is approximated by:

$$h_{IP} = cos(\beta)(R_N + h) - R_N \tag{97}$$

where R_N is defined by Equation 56.

Through h_{IP} and considering $el = 0$ it is possible to calculate the effect T at IP by using the equations shown before.
The computation of the desired effect at user position T_U is assumed (by geometry) as proportional to T accounting for the distance y between IP and the user position:

$$\begin{aligned} x &= \sqrt{(R_N + h_T)^2 - (R_N + h_{IP})^2} \\ y &= \sqrt{(R_N + h)^2 - (R_N + h_{IP})^2} \end{aligned} \tag{98}$$

where h_T shall be replaced by hw or hd.

$$T_U = \left(1 + \frac{y}{x}\right) T \tag{99}$$

3. User outside dry/wet troposphere

In this case the user can still be reached by signals whose elevation angle has a value below of that defined for the troposphere layer el_T, then passing through it. The effect in this case can be computed in a similar way as done before, but using an effect calculation point ECP, as done for the ionosphere, and its related elevation el_{ECP} as basis, which is defined in the near user intersection of the path with the troposphere

layer in question (See Figure 27). From this point on, everything is computed as the user were in this point.

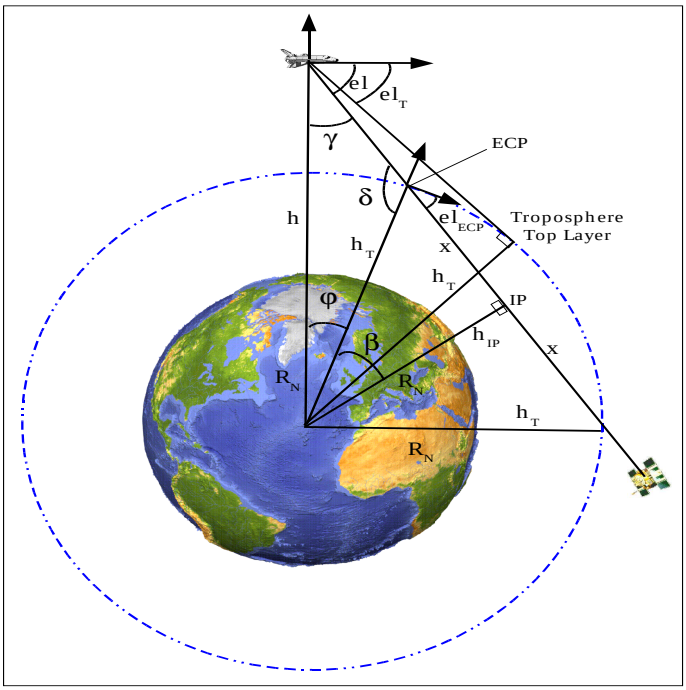

Figure 27: Tropospheric path delay for users outside the troposphere.

The ECP calculation process is the same as shown for ionosphere but considering tropospheric heights.

$$el_T = -arccos\left(\frac{R_N + h_T}{R_N + h}\right) \tag{100}$$

Through h_{IP} and considering $el = 0$ it is possible to calculate the effect T in ECP by using the equations shown before. Note that in this case both x and y distances would be the same, thus the computation of the desired effect at user position T_U is assumed (by geometry) as twice the effect T

$$T_U = 2T \tag{101}$$

All the considerations shown above must be taken for both dry and wet troposphere with their respective layer heights (Equation 94).

The following figures show the tropospheric path delay effect examples for different situations at user geodetic angles $\phi_G = 0^o$ and $\lambda_G = 0^o$.

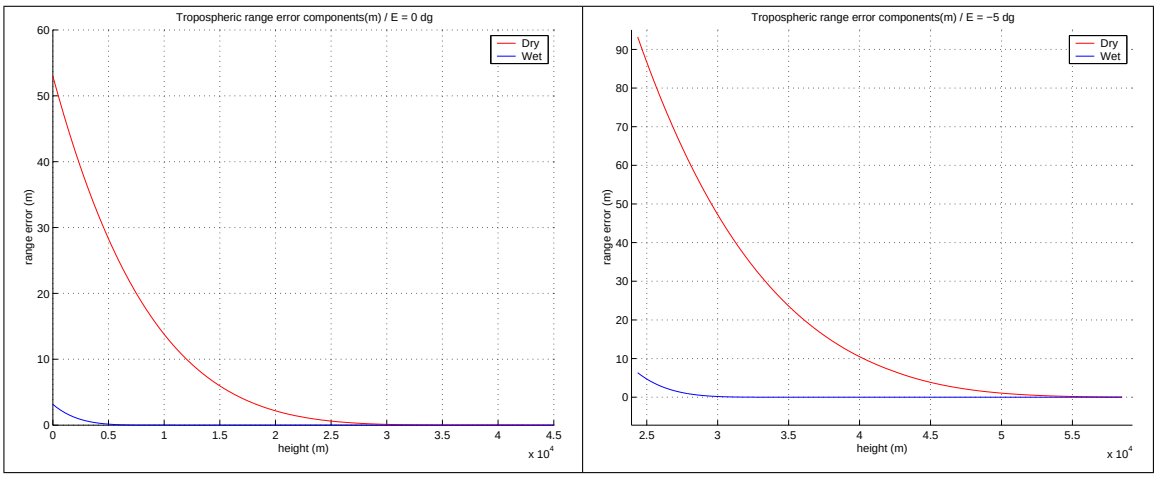

Figure 28: Tropospheric path delay for different elevations. User at (lat=0, lon=0).

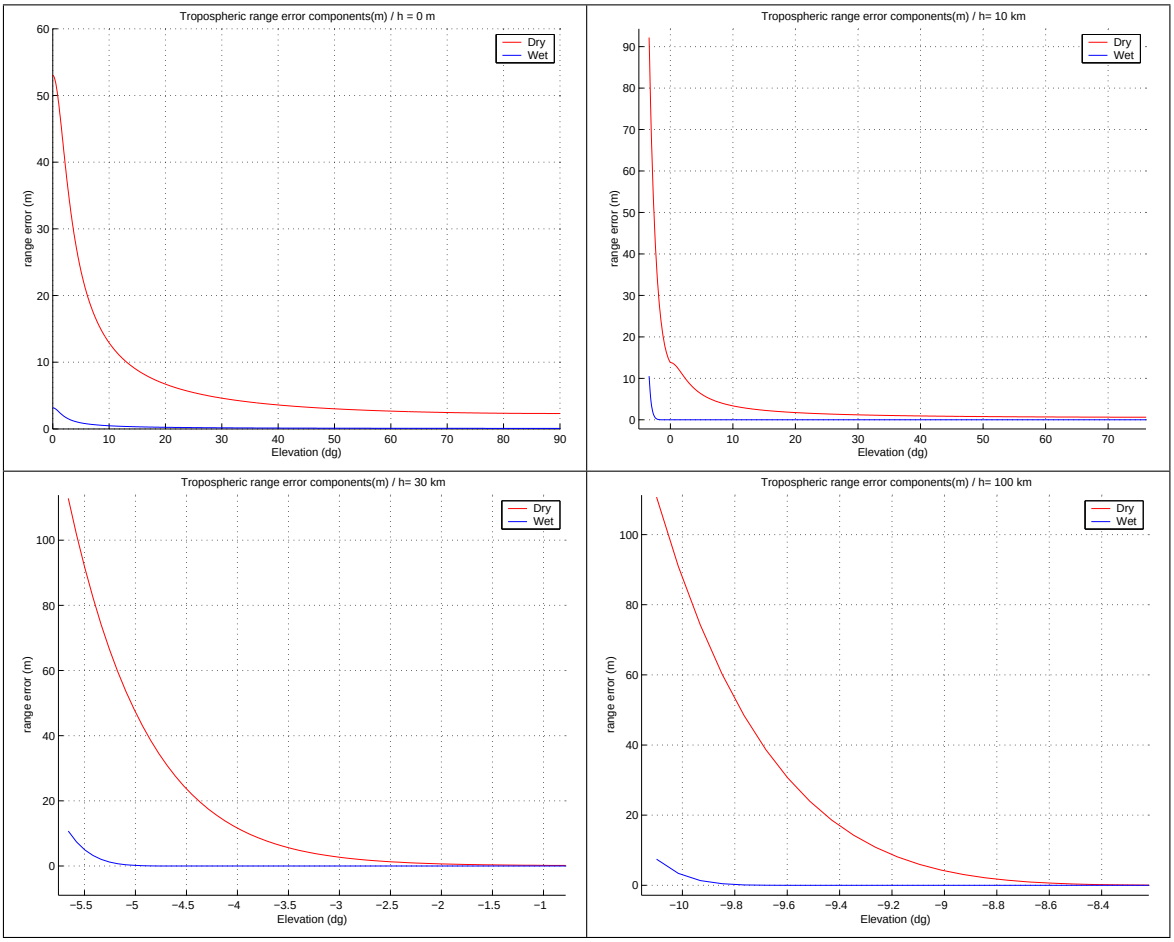

Figure 29: Tropospheric path delay for different heights. dg=degrees. User at (lat=0, lon=0).

From the figures it is possible to realize that the influence from dry component is about 90% while that from the wet part is about 10%.

6.5. Multipath correction

With GPS, multipath occurs when the signal bounces off a building or terrain before reaching the GPS receiver's antenna. These signals takes longer to reach the receiver than if it had travelled a direct path. As a result multiple copies of the transmitted signal are present in the tracking loop of the receiver. The tracking loop tries to track the resulting sum of the multiple signals which are masking the real correlation peak. This causes errors in the time-of-arrival estimation i.e. makes the GPS receiver think the satellite is farther away than it really is. This adds error to the overall position determination.

The first line of defense is to use a combination of antenna cut-off angle and a good antenna location to minimize the problem of multipath. A second approach is to use so-called narrow correlatorreceivers which tend to minimize the impact of multipath on range tracking accuracies. In kinematic applications, such the background for this simulator, multipath behaves more randomly because the movement of the vehicle and that the surface changes the reflecting geometry in a relatively random way. Multipath errors are also unique for each receiver, and uncorrelated between signals. Therefore, it is a very difficult problem to calculate multipath error. Because of this, is only the error due to one surface reflection taken into concern in the simulation. The reflection is the one from Earth surface for a vehicle/receiver at height h.

If the satellite elevation angle is E, the reflected ray is delayed by $\Delta\tau$ with respect to the direct ray by $\Delta R = c\Delta\tau = 2h\sin(E)$.

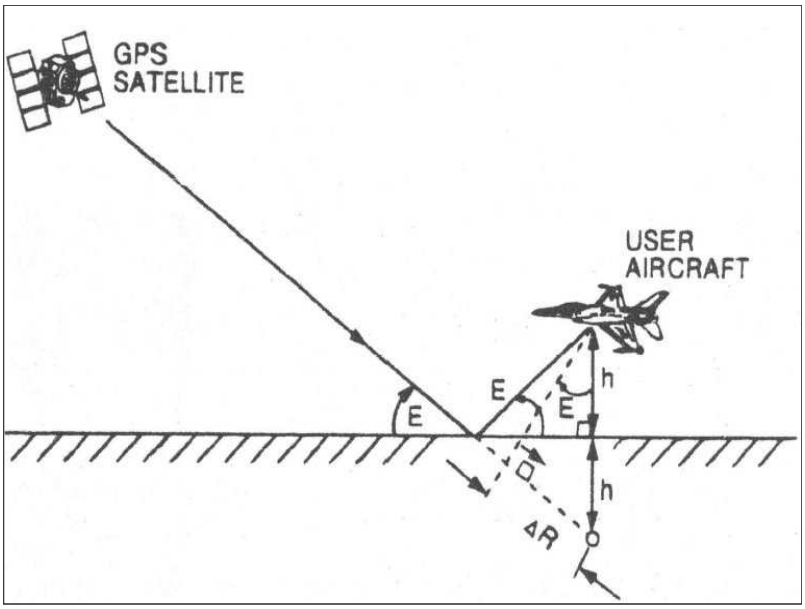

Figure 30: Multipath delay varies with elevation angle E and user altitude h.

The reflected signal amplitude from the Earth surface can be nearly as large and sometimes even larger than the direct ray. To distinguish which ray that are the correct one

GPS receiver 'can' reject multipath signals if the differential delay $\Delta\tau > 1.5\mu s$ for the C/A code and 0.15 μs for the P(Y)-code ([13]). Note the region of potential multipath delay problems for the C/A code is then:

$$1.5\mu s > \frac{2h}{c}\sin(E) = \Delta\tau \qquad or \qquad h\sin(E) < (1.5\mu s)c = 448.5m \tag{102}$$

Note that Earth is approximated to be flat. The rejection of multipath at 0.15 μs is not entirely truth, reference [13] (p.559); *The relative delay of the multipath is a function of receiver-to-object distance and proximity of the object to the satellite-to-receiver line-of-sight. The closer an object is to the line-of-sight, the greater the receiver-to-object distance can be while still yielding a relative multipath delay of less than 1.5chips. The conclusion, then, is that increased receiver-to-object distance only guarantees a weakening of the multipath signal*

Although the argument above, the multipath has been included in the simulation. Decision of the multipath efficiency will be taken after verification of the simulation program.

7. Verification and Conclusions

The verification of the developed simulation program was performed by comparing the simulated parameters/results with the used receiver parameters/results, using same input. To do this the hardware code in the GPS receiver was extended to store its calculated and used parameters in data files. This is the same way the NAV-message with Ephemeris, Almanac, UTC and Ionospheric parameters where stored. After the hardware code had been extended to store the parameters of interest, following verification procedure was performed:

1. Run the GPS receiver, collect received data and store calculated parameter in file.
2. Run the simulation program, based on the collected/stored data (NAV-message).
3. Compare the stored parameters/results from the GPS receiver with the simulation parameters/results.

Many problems were found, mostly related to the calculation of the *GPS system time* and had to be fixed. But the final result was satisfied. Compared with the receiver, the difference in calculating the geometric range is less than 0.01m and the background of this is a very small difference in the *GPS time*. The origin of this was not found but as it is so small it could be a difference in chosen constants. Table 7 shows the difference of some simulated parameters compared with the receiver result, simulated from Ephemeris data. The difference between simulated Almanac data and the receiver result are not shown because the accuracy of Almanac data is depending on its age, i.e. if the time of the Almanac data since transmission (from MCS) is one day the accuracy is 900m. Direct comparison between a receiver calculation (based on Ephemeris data) with simulated Almanac data is possible just by requesting the simulation time to correspond to the ephemeris, but for verification purposes it is not recommended since Almanac data are approximations and gives low precise results for satellite position.

Parameter	**Difference**
Calculated GPS Time	$< 1.3 \cdot 10^{-7}\ s$
Geometric Range	$< 1 \cdot 10^{-2}\ m$
Ionospheric Range Error	$< 3.6\ m$
Tropospheric Range Error	$< 0.6\ m$
Satellite Clock Range	$< 0.2\ m$

Table 7: Simulation difference for Ephemeris data with respect to used GPS receiver (one time step).

As one can see in the table above, the biggest calculation difference lay on the *ionospheric range error*. This difference is because, although both the simulation and receiver are using Klobuchar's ionospheric model, there is a difference in the procedure of calculating the intermediate point. In the receiver's calculation there exists approximations on it, which the simulation does not use and it is because of this the simulation disagree from the receiver result.

There were no way to check the multipath function, since the receiver does not calculate it. Since the multipath model here was too basic (only one flat bounce surface was included), it only covers the effect due to Earth surface. Also a spaceborne receiver won't suffer for extreme multipath delay since there are less near objects for a signal to bounce on.

The simulated signal to noise ratio could neither be compared. This because the receivers calculation of it was based on information from the tracking loop and not from a hardware code. The signal to noise ratio simulation use also a theoretical model which mostly changed with the distance and angle to the satellite. Because of this became the difference between good and bad signals very small. One way to get a more precise SNR value, is to have more accurate information about the transmitted power on every GPS satellite, this since the antenna power output could differ up to 6dB between GPS satellites.

The verification of the visibility model for the antenna and the model for Earth shadow showed that they worked very well. This verification was first based on comparison between which satellites that where visual for the receiver and simulated satellite visibility (check if same satellites are visual). Second was the visual check that the simulation gave, (see figure 31 and 32). The visibility verification of the antenna model was done by changing the direction of a narrow receiver antenna beam and graphically viewing the result.

The two figures 31 and 32 shows a simulation of all satellites made from Almanac data. The red star is the receiver position, the blue dots are visible satellites and green dots are nonvisible satellites.

Note that if this simulation program is used in a application there the receiver antenna or the body is moving all calculations are needed to be redone and then based on new receiver input values.

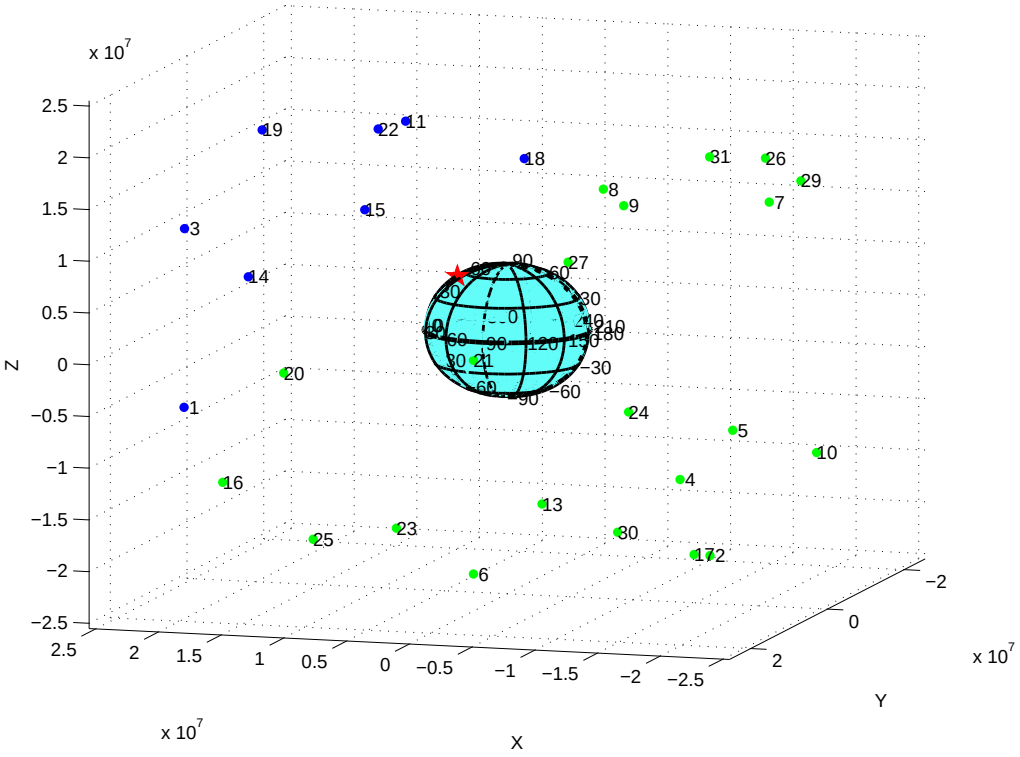

Figure 31: 3D view of simulation from Almanac data. One time step. The XYZ coordinate system is in the ECEF reference frame and the unit is meters.

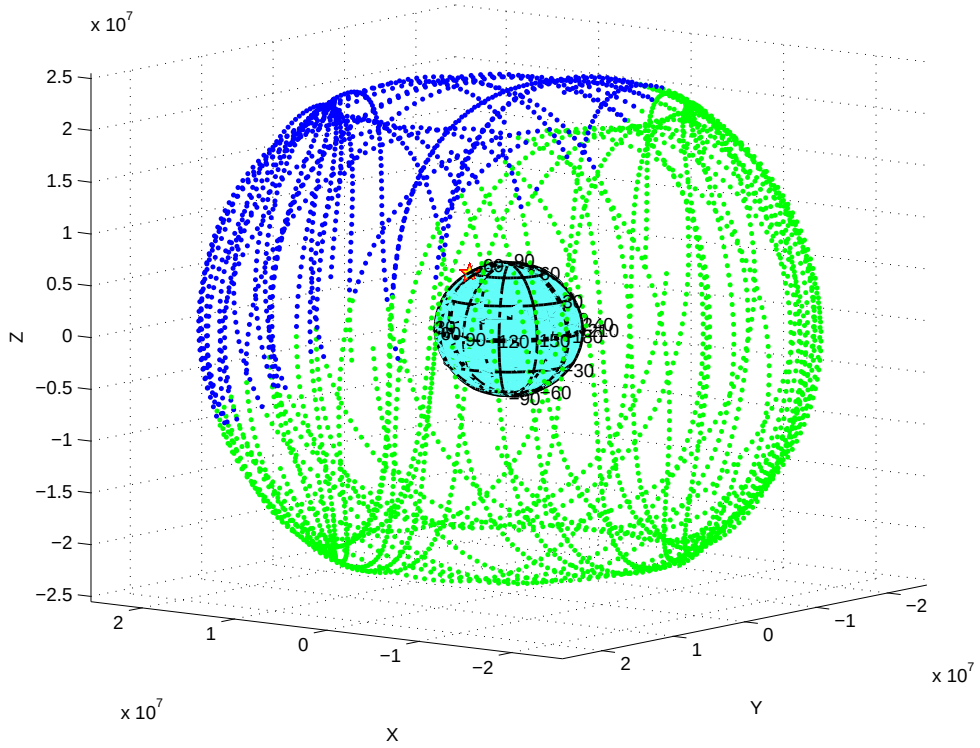

Figure 32: 24 hour orbit simulation from Almanac data. The XYZ coordinate system is in the ECEF reference frame and the unit is meters.

7.1. Outlook

This simulation program is a static simulation, i.e. it only calculates satellites position for a given time and from that calculates the pseudo range to the receiver. This means that it does not calculate the receivers velocity which would give a more accurate navigation model. This is left for later investigation and implementation.

When one simulates with Ephemeris data, only the satellites that are visible for the receiver antenna can be collected and then a precise simulation for these satellite can be made. To perform a precise simulation with all GPS satellites using Ephemeris data one must collect data from different times until all GPS satellite have been visible for the receiver antenna. The simulation program can not handle different GPS times today and therefore can not collect different Ephemeris data to be used. This feature would increase the simulation reliability and is recommended to be implemented.

The Ephemeris data collection problem discussed above can be solved if one download the data from internet. But it have not been checked up if there exist any web pages with needed parameters therefore have this solution not been tested.

8. Bibliography

References

[1] Peter Berlin. *Satellite Platform Design*. 1st edition, 2004.

[2] G. B. Carvalho. Reference Frame Definitions. Technical Report INT-GEN-DF-ZAR-001, ZARM Bremen, November 2003.

[3] G. B. Carvalho. Practical Approaches to the Global Positioning System. Technical Report INT-GPS-TN-ZAR-001, ZARM, September 2004.

[4] Phillip Martin Corbell. Design and validation of an accurate GPS signal and receiver truth model for comparing advanced receviers processing techniques. Master's thesis, March 2000.

[5] Lei. Dong. IF GPS Signal Simulator Development and Verification. Master's thesis, December 2003.

[6] Eurocontrol, IfEN. *WGS 84 Implementation Manual*.

[7] J. Farrel and M. Barth. *The Global Positioning System and Inertial Navigation*. McGraw-Hill, 1998.

[8] Mohinder S. Grewal, Lawrence R. Weill, and Angus P. Andrews. *Global Positioning Systems, Inertial Navigation and Integration*. John Wiley & Sons, Inc., 2001.

[9] B. Hofmann-Wellenhof, H. Lichtenegger, and J. Collins. *GPS Theory and Practice*. Springer-Verlag Wien New York, August 2000.

[10] Elliott D. Kaplan. *Understanding GPS, Principles and Applications*. 1996.

[11] J.A. Klobuchar. Ionospheric Time-Delay Algorithm for Single-Frequency GPS Users. Technical Report 3, 1987.

[12] Garmin Ltd. What is GPS?, 2004. http://www.garmin.com/aboutGPS/.

[13] B.W. Parkinson and J.J. Spilker Jr. *Global Positioning System: Theory and Applications Volume I*. Progress in Astronautics and Aeronautics, Vol. 163. AIAA, 1996.

[14] L. Råde and B. Westergren. *Mathematics Handbook for Science and Engineering*. Studentlitteratur, 4th edition, 1998.

[15] J.R. Wertz, editor. *Spacecraft Attitude Determination and Control*. Kluwer Academic Publishers, Dordrecht, The Netherlands, 1978.

[16] Wikipedia. Geodesy, 2004. http://en.wikipedia.org/wiki/Geodesy.

A. Physical Constants

The Earth WGS-84 (World Geodetic System-1984) model parameters are:

Definition	Value
Earth mass (M_E)	5.9742×10^{24} (kg)
Earth semimajor axis (A_E)	6378137.0 (m)
Earth semiminor axis (B_E)	6356752.3142 (m)
Earth geoid eccentricity (e_E)	0.08181919
Earth turn rate (ω_E)	$7.2921151467 \times 10^{-5}$ (rad/s)
Earth gravitational constant (μ_E)	$3.986004418 \times 10^{14}$ (m^3/s^2)

Table 8: WGS-84 definitions.

Other physical constants ([15]):

Definition	Value
Speed of light in vacuum (c)	299792458 (m/s)
Universal gravitational constant (G)	6.6720×10^{-11} $(m^3/(kg \cdot s^2))$
Bolzmann Constant (k)	1.380658×10^{-23} $(J/K))$

Table 9: Physical constants.

Standard atmosphere at sea level

Definition	Value
Mean Pressure (P)	101.3 (kPa)
Mean Temperature (T)	15 $(Celcius)$
50% Humidity (e)	0.85 (kPa)

Table 10: Standard atmosphere constants.

Mathematical constants:

Definition	Value
π	3.1415926535898

Table 11: Mathematical constants.

B. Reference Frames and position transformation

This appendix is compiled from [2]. Reference frames are thought to give three-dimensional representations a reference. A Reference frame is a set of right-handed orthogonal axes XYZ completely situated in the three-dimensional space related to a set, a group, of references. A reference frame can be used with different coordinate systems.

B.1. Inertial Reference Frames

Inertial reference frames are based in references, which can be considered static in relation to the distant stars (considered also static). Actually there are no absolutely static references in universe, but for general space applications, some quasi-inertial references are treated as inertial in order to allow the definition of inertial reference frames. Hence the inertial reference frames can be considered as fixed to the distant stars, that means, the axes keep their directions related to other movements and rotations (Earth's orbit and rotation for example).
Before the definition of the inertial reference frames take place, some definitions are needed:

- Celestial meridian - defined as the observer's zenith meridian.
- Hour angle - defined as the angle between celestial meridian and the specified meridian, measured at Earth's equatorial plane.
- Earth's rotation axis - Earth's mean rotation axis neglected nutation, precession and minor changing effects.
- Earth's equatorial plane - Plane orthogonal to the Earth's rotation axis, which divide the Earth in two hemispheres.
- Ecliptic plane - Earth's orbital plane around the Sun neglected changing effects.
- Vernal equinox (γ) - direction from Earth to the Sun in the intersection between Earth's equatorial plane and Ecliptic plane at the instant that the Sun crosses upward, from Southern to the Northern Earth hemisphere. This time defines the beginning of Spring in Northern hemisphere.
  Because Earth's rotation axis changing effects (consequent changes also in equatorial plane), this reference is changing slowly ($5 arcsec/year$). Thus a static reference direction was defined by J2000.0 system taking the vernal equinox at the date of 12:00:00 GMT, january 1st, 2000.

B.1.1. Earth Centered Inertial Reference Frame

Given a right-handed orthogonal set of three axes XYZ, the cartesian ECI (Earth-centered inertial) reference frame is a geocentric frame defined as:

- Origin in the Earth's center of mass.
- X_{ECI} axis pointing in the direction of the vernal equinox γ.
- Z_{ECI} axis pointing in the positive sense in direction of the Earth's rotation axis (North Pole).
- Y_{ECI} axis completing the right-handed orthogonal axes set.

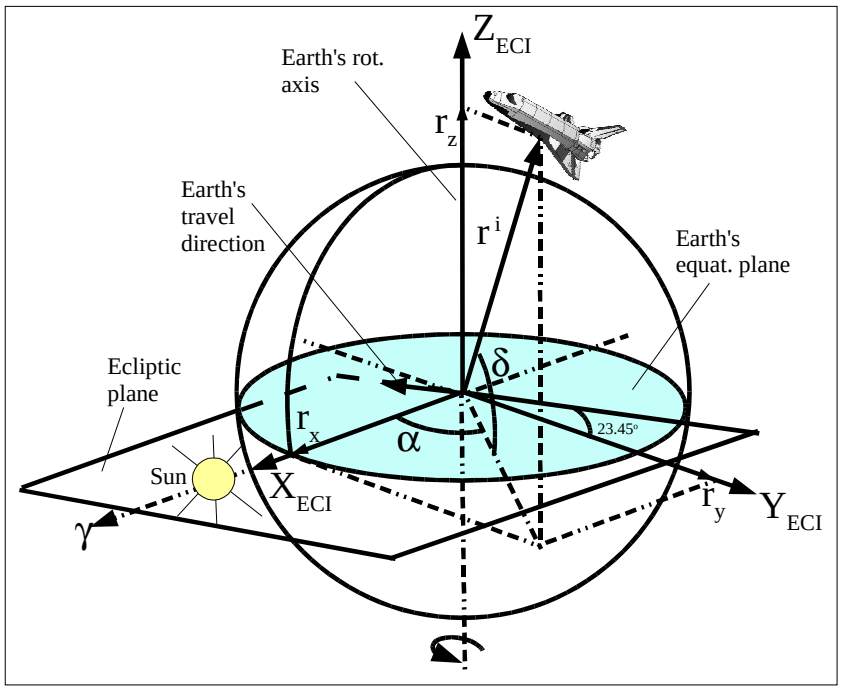

Figure 33: ECI coordinate frame.

The polar coordinates defined for the ECI frame are:

- Origin in the Earth's center of mass.
- right-ascension α - the Hour angle defined between the vector and the X_{ECI} axis, positively defined in counter-clockwise sense.
- declination δ - the angle defined between the vector and its orthogonal projection in XY plane, positively defined in counter-clockwise sense
- radius r - the vector modulus

B.2. Fixed Reference Frames

Fixed reference frames are based in references, which are fixed to a given rigid body. This rigid body can be anything, for example: The Earth, a planet, a spacecraft, an aircraft. Note that these examples are not rigid bodies in a strict sense, but they can be thought as rigid using a simplification model. Fixed reference frames are not fixed to other references that do not belong to the same rigid body to which it is attached to. That means, the axes change their directions related to movements external to the rigid body scope.

B.2.1. Earth Centered, Earth-fixed Reference Frame

The $ECEF$ (Earth-centered, Earth-fixed) is a coordinate frame fixed to the Earth, what means it accompanies the Earth's rotation. Given a right-handed orthogonal set of three axes XYZ, the cartesian $ECEF$ reference frame is a geocentric frame defined as:

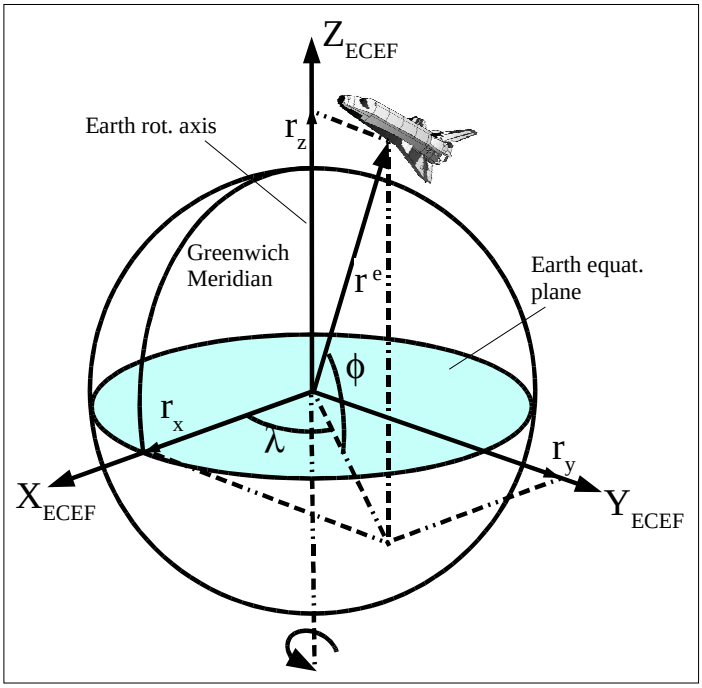

Figure 34: ECEF coordinate frame.

- Origin in the Earth's center of mass.
- X_{ECEF} axis - axis pointing in the direction of Earth's prime meridian (Greenwich) at the Earth's equator.
- Z_{ECEF} axis - axis pointing in the positive sense in the direction of the Earth's rotation axis (North Pole).
- Y_{ECEF} axis - axis completing the right-handed orthogonal axes set.

The polar coordinates defined for the $ECEF$, also known as geocentric coordinates, are:

- Origin in the Earth's center of mass.
- longitude λ - the Hour angle defined between the vector and the X_{ECEF} axis, positively defined in counter-clockwise sense.
- declination ϕ - the angle defined between the vector and its orthogonal projection in XY plane, positively defined in counter-clockwise sense
- radius r - the vector modulus

B.2.2. The Geodetic Reference Frame

$WGS-84$ is the 1984 revision of the World Geodetic System. It defines a earth fixed global reference frame, for use in geodesy and navigation and will be valid up to about 2010, ([16]). It includes an earth model which is defined by a set of primary and secondary parameters. The reference frame is coordinated in XYZ or in (ϕ,λ, h), where the parameter h is the (geometric) height above the $WGS-84$ ellipsoid. The primary parameters define the shape of an earth ellipsoid, its angular velocity, and the earth mass which is included in the ellipsoid reference. The Secondary parameters define a detailed gravity model of the earth. Each datum has been produced by fitting a particular mathematical Earth model (ellipsoid) to the true shape of the Earth (geoid) in such a way as to minimize the differences between the ellipsoid and the geoid over the area of interest.

Thus, for the Geodetic reference frame, a point in space can be defined by (ϕ,λ, h):

- ϕ_G - the angle defined between the equatorial plane and the normal to the reference ellipsoid surface that passes through the point indicated by the geocentric coordinates (λ, ϕ) over the reference ellipsoid (see Figure 35). It is positively defined in counter-clockwise sense.
- λ_G - the angle defined between the vector orthogonal projection in XY plane and the X_{ECEF} axis, positively defined in counter-clockwise sense
- r - the vector modulus

The geodetic longitude ϕ_G is exactly the same as in $ECEF$, but the geodetic latitude λ_G is different from its correspondent spherical latitude. Thus, the Geodetic longitude is simply treated as λ, while the Geodetic latitude can differ from geocentric latitude by as much as 12 arc-minutes, which means at about 20km of northing distance.

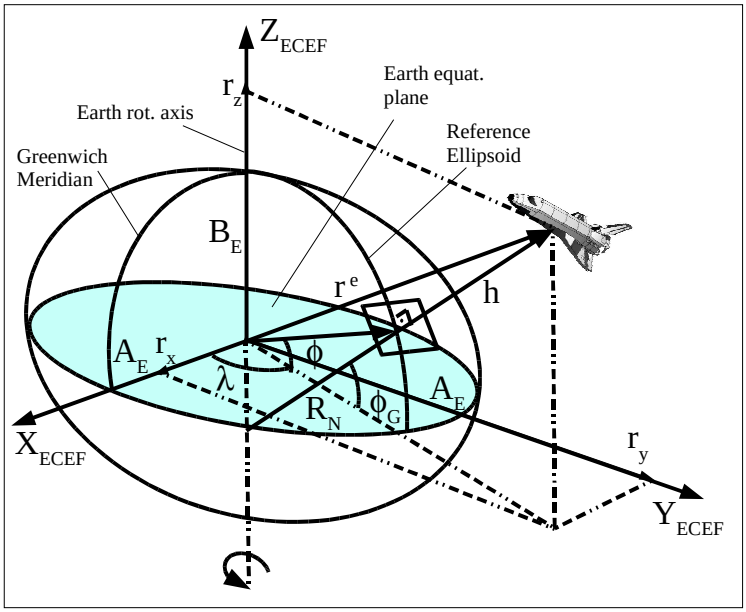

Figure 35: Geodetic reference frame.

B.2.3. Local Tangent Plane Reference Frames

The Local Tangent Plane (LTP) reference frame, also known as local level frame, represent the Earth as being locally flat. However, it is centered in the vehicle, instead of being related to Earth center. It serves as local reference direction for a vehicle operation near to the surface of the Earth.

B.2.3.1. North-East-Down Reference Frame

Given a right-handed orthogonal set of three axes XYZ, the NED (North-East-Down) reference frame is defined as:

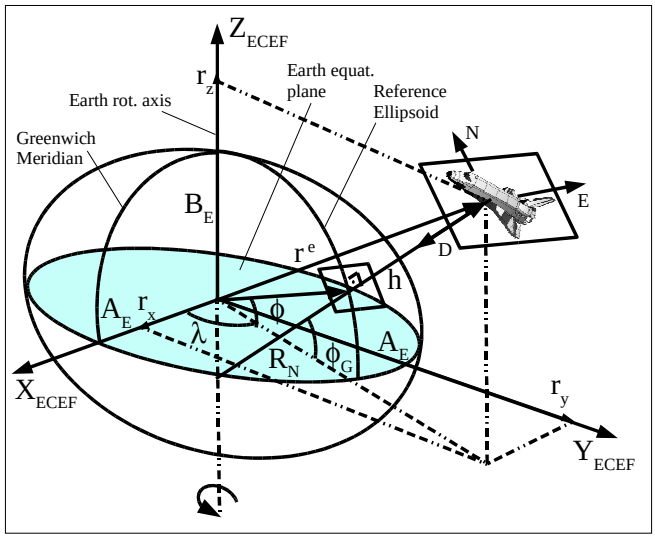

Figure 36: NED reference frame.

- Origin located at the computed specific force origin.
- N axis (X_{NED}) - axis pointing toward in the direction of increasing latitude (geographic North), in the plane parallel to a plane that is tangent to the reference ellipsoid at the geodetic location of the vehicle.
- E axis (Y_{NED}) - axis pointing toward in the direction of increasing Longitude, (geographic East), in the plane parallel to a plane that is tangent to the reference ellipsoid at the geodetic location of the vehicle.
- D axis (Z_{NED}) - axis pointing downward in the direction of local ellipsoid vertical.

B.2.3.2. East-North-Up Reference Frame

Given a right-handed orthogonal set of three axes XYZ, the ENU (East-North-Up) reference frame is defined as:

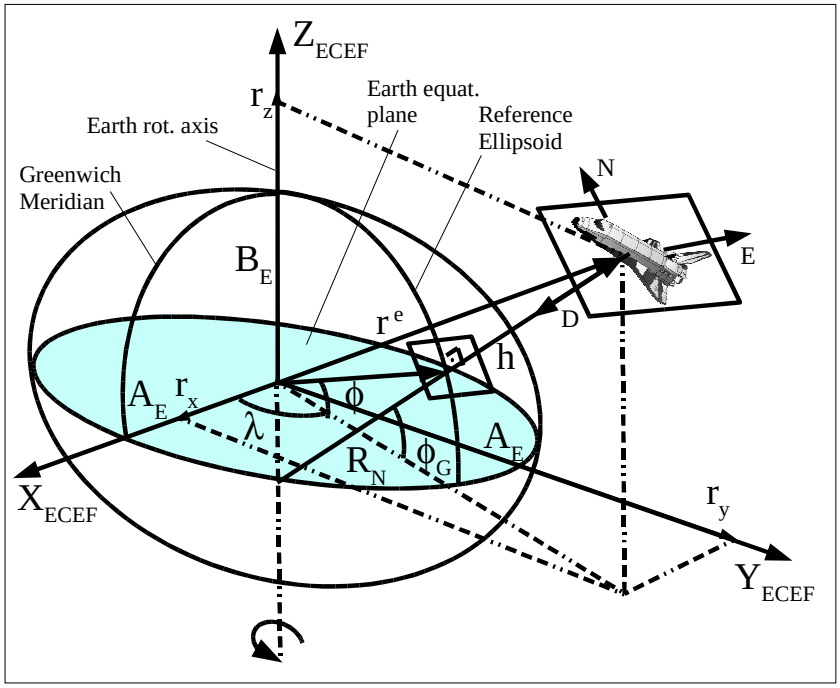

Figure 37: ENU reference frame.

- Origin located at the computed specific force origin.
- E axis (X_{ENU}) - axis pointing toward in the direction of increasing Longitude, (geographic East), in the plane parallel to a plane that is tangent to the reference ellipsoid at the geodetic location of the vehicle.
- N axis (Y_{ENU}) - axis pointing toward in the direction of increasing latitude (geographic North), in the plane parallel to a plane that is tangent to the reference ellipsoid at the geodetic location of the vehicle.

- U axis (Z_{ENU}) - axis pointing upward in the direction of local ellipsoid vertical.

B.3. ECI to ECEF transformation

The difference between ECI and ECEF lies on that while ECI is fixed to the distant stars, the ECEF accompanies the Earth's rotation. All other references stay. This results that they are simply related by the sidereal time angle α_E as shown in figure 38.

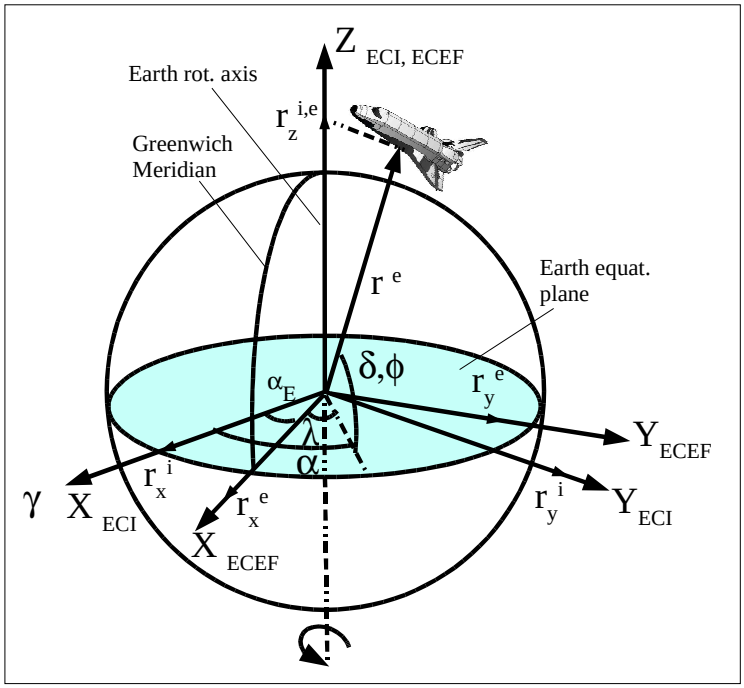

Figure 38: ECI x ECEF reference frame.

The sidereal time angle α_E is right-ascension of the X_{ECEF} and can be described in function of the current Date and UTC time. The transformation between both ECI and ECEF can be accomplished through the rotation around Z_{ECI} axis through the rotation matrix $\underline{\underline{T}}_i^e$, which represents the Earth's turn:

$$\underline{\underline{T}}_i^e(\alpha_E) = \begin{bmatrix} cos(\alpha_E) & sin(\alpha_E) & 0 \\ -sin(\alpha_E) & cos(\alpha_E) & 0 \\ 0 & 0 & 1 \end{bmatrix} \tag{103}$$

Hence, the transformation between ECI and ECEF vectors is:

$$\underline{r}^e = \underline{\underline{T}}_i^e(\alpha_E) \cdot \underline{r}^i, \quad \underline{r}^i = \underline{\underline{T}}_i^e(\alpha_E)^T \cdot \underline{r}^e \tag{104}$$

The relations between the polar angles in ECI and ECEF are:

$$\phi = \delta, \quad \alpha = \alpha_E + \lambda \tag{105}$$

B.4. ECEF to Geodetic transformation

The relations between Cartesian ECEF and Geodetic coordinates are ([7]):

$$r_x^e = (R_N + h)cos\phi_G \; cos\lambda \tag{106}$$

$$r_y^e = (R_N + h)cos\phi_G \; sin\lambda \tag{107}$$

$$r_z^e = (R_N(1 - e_E^2) + h)sin\phi_G \tag{108}$$

where

$$R_N = \frac{A_E}{\sqrt{1 - e_E^2 sin^2\phi_G}} \tag{109}$$

is the length of the normal from the ellipsoid surface to its intersection with Z_{ECEF}.

The inverse transformation can only be given explicitly for the longitude:

$$\lambda = atan2\left(r_y^e, r_x^e\right) \tag{110}$$

where $atan2$ is the four-quadrant $arctan$ function, while for the latitude, iteration would be needed. To avoid iterations and complicated algorithms a approximated closed-form algorithm can be adopted [7]:

$$r_{xy}^e = \sqrt{r_x^{e\ 2} + r_y^{e\ 2}} \tag{111}$$

$$e'_E = \frac{A_E \cdot e_E}{B_E} \tag{112}$$

$$\phi_G = atan\left(\frac{r_z^e + (e'_E)^2 B_E \; sin^3\theta}{r_{xy}^e - e_E^2 A_E \; cos^3\theta}\right) \tag{113}$$

$$h = \begin{cases} \frac{r_{xy}^e}{cos\phi_G} - R_N, \phi_G \leq \pi/4 \\ \frac{r_z^e}{sin\phi_G} - R_N(1 - e^2), \phi_G > \pi/4 \end{cases} \tag{114}$$

where

$$\theta = atan2(r_z^e A_E, r_{xy}^e B_E) \tag{115}$$

For h and ϕ_G the following accuracies can be adopted:

$$\varepsilon_h < 1.5 \cdot 10^{-3} m \text{ and } \varepsilon_{\phi_G} < 1.2 \cdot 10^{-3} m \text{ for } h < 400km \tag{116}$$

$$\varepsilon_h < 2 \cdot 10^{-5} m \text{ and } \varepsilon_{\phi_G} < 1.5 \cdot 10^{-5} m \text{ for } h < 40km \tag{117}$$

$$\varepsilon_h < 2 \cdot 10^{-7} m \text{ and } \varepsilon_{\phi_G} < 1.5 \cdot 10^{-7} m \text{ for } h < 4km \tag{118}$$

The constants e_E, A_E, B_E can be found in Appendix A.

B.5. Transformation matrix between ECEF and NED/ENU Reference Frame

The transformation between ECEF and NED reference frames can be obtained through an Euler 3-2-1 rotation (see Appendix C.2), with first rotation around Z_{ECEF} axis with λ, second rotation around the resulting Y axis with $-(\phi_G + \pi/2)$ and third rotation around the resulting X axis with 0 rad through the rotation matrix $\underline{\underline{T}}_e^n(\phi_G, \lambda)$:

$$\underline{\underline{T}}_e^n(\phi_G, \lambda) = \begin{bmatrix} -sin\phi_G\ cos\lambda & -sin\phi_G\ sin\lambda & cos\phi_G \\ -sin\lambda & cos\lambda & 0 \\ -cos\phi_G\ cos\lambda & -cos\phi_G\ sin\lambda & -sin\phi_G \end{bmatrix} \tag{119}$$

The fact that the origin of NED frame NED_0^e described in ECEF is different from the ECEF origin must also be taken into account. Furthermore, the ϕ_G and λ angles must be defined from the NED_0^e coordinates. Hence, a transformation between ECEF and NED vectors is:

$$\underline{r}^n = \underline{\underline{T}}_e^n(\phi_G, \lambda) \cdot (\underline{r}^e - NED_0^e), \quad \underline{r}^e = \underline{\underline{T}}_e^n(\phi_G, \lambda)^T \cdot \underline{r}^n + NED_0^e \tag{120}$$

The transformation between ENU and NED reference frames can be obtained through an Euler 3-2-1 rotation (see Appendix C.2), with first rotation around Z_{ENU} axis with $-\pi/2$ rad, second rotation around the resulting Y axis with π rad and third rotation around the resulting X axis with 0 rad, which corresponding rotation matrices $\underline{\underline{T}}_u^n = \underline{\underline{T}}_n^u$ are:

$$\underline{\underline{T}}_u^n = \underline{\underline{T}}_n^u = \begin{bmatrix} 0 & 1 & 0 \\ 1 & 0 & 0 \\ 0 & 0 & -1 \end{bmatrix} \tag{121}$$

Hence, a transformation between ENU and NED vectors is:

$$\underline{r}^n = \underline{\underline{T}}_u^n \cdot \underline{r}^u, \quad \underline{r}^u = \underline{\underline{T}}_n^u \cdot \underline{r}^n \tag{122}$$

C. Transformations among Reference Frames

This appendix is compiled from [2]. Transformations among Reference Frames are methods for transforming a vector represented in one reference frame into the appropriate representation in another reference frame.

C.1. Euler axis-angle definition

The Euler axis-angle is used to define a reference frame transformation in terms of a specified set of a three dimensional axis $\hat{\underline{e}}$ with a rotation angle ϕ around it. With such a set, any three dimensional rotation can take place.

C.2. Euler angles

Euler angles are used to define a reference frame transformation in terms of a set of three angular rotations performed in a specified sequence around three specified orthogonal right-handed axes.
The rotation angles are (ϕ, θ, ψ) in this sequence, which can be used to represent a rotation in each of the three-dimensional axes XYZ. Thus, to specify the rotation sequence, the axes are named $X = 1$, $Y = 2$ and $Z = 3$.
With such a set, there are 12 possible rotation sequences, where the rotation sequence is defined as 1-2-3, 1-3-2, 3-2-1, and so on.
For example, the sequence 3-2-1 means that (see Figures 39, 40 and 41):

- the first rotation ϕ will be done around the axis Z (3).
- the second rotation θ will be done around the axis Y (2).
- the third rotation ψ will be done around the axis X (1).

C.2.1. Time-Derivative of Euler angles Algebra

If Euler angles represent the attitude of a rotating rigid body b related to frame a, its derivative with respect to time is needed for propagation. For the attitude of body b with respect to the reference frame a the transformation can be expressed by (ϕ, θ, ψ) in a defined Euler sequence. The angular velocity of b with respect to frame a, measured in the frame b, is expressed as $\underline{\omega}^b_{a,b}$.
Thus it is necessary to find the relations between the attitude-rate Euler angles $\dot{\phi}$, $\dot{\theta}$ and $\dot{\psi}$, in a specified rotation sequence, and the body angular velocity $\underline{\omega}^b_{a,b}$ measured in b. As an example, the desired relation is shown for the 3-2-1 rotation sequence.

In the following figures, the 3-2-1 rotation sequence is shown, where the frame a is represented by the XYZ axes while b by the $(XYZ)'''$ axes.
This rotations, which take a vector in the frame a and bring to the frame b, result in the attitude of b related to a.
Thus, the angular velocity vector $\underline{\omega}^b_{a,b}$ measured in b can be represented as $[\omega'''_x \ \omega'''_y \ \omega'''_z]^T$.

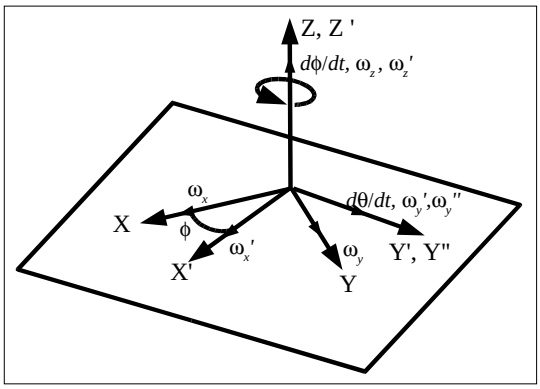

Figure 39: First rotation around axis Z(3).

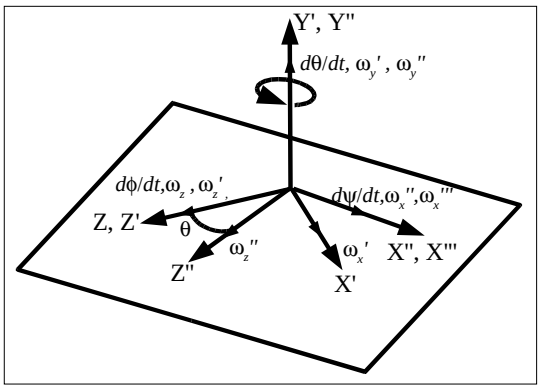

Figure 40: Second rotation around axis Y(2).

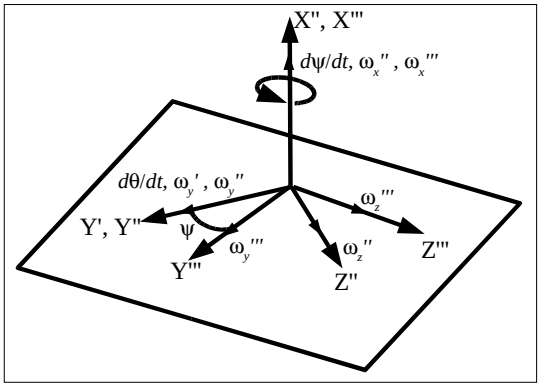

Figure 41: Third rotation around axis X(1).

From the previous figures, it is possible to observe that:

$$\frac{d\phi}{dt} = \omega_z = \omega_z', \quad \frac{d\theta}{dt} = \omega_y' = \omega_y'', \quad \frac{d\psi}{dt} = \omega_x'' = \omega_x''' \tag{123}$$

To find the relations among the Euler angle-rates $\dot{\phi}$, $\dot{\theta}$ and $\dot{\psi}$ and the body angular velocities $[\omega_x''' \ \omega_y''' \ \omega_z''']^T$, it is necessary to find the relations back to $[\omega_x \ \omega_y \ \omega_z]^T$. The relations among each frame in the sequence step are:

$$\text{First Rotation (Z):} \quad \begin{bmatrix} \omega_x \\ \omega_y \\ \omega_z \end{bmatrix} = \begin{bmatrix} cos\phi & -sin\phi & 0 \\ sin\phi & cos\phi & 0 \\ 0 & 0 & 1 \end{bmatrix} \begin{bmatrix} \omega_x' \\ \omega_y' \\ \omega_z' \end{bmatrix} \tag{124}$$

$$\text{Second Rotation (Y):} \quad \begin{bmatrix} \omega_x' \\ \omega_y' \\ \omega_z' \end{bmatrix} = \begin{bmatrix} cos\theta & 0 & sin\theta \\ 0 & 1 & 0 \\ -sin\theta & 0 & cos\theta \end{bmatrix} \begin{bmatrix} \omega_x'' \\ \omega_y'' \\ \omega_z'' \end{bmatrix} \tag{125}$$

$$\text{Third Rotation (X):} \quad \begin{bmatrix} \omega_x'' \\ \omega_y'' \\ \omega_z'' \end{bmatrix} = \begin{bmatrix} 1 & 0 & 0 \\ 0 & cos\psi & -sin\psi \\ 0 & sin\psi & cos\psi \end{bmatrix} \begin{bmatrix} \omega_x''' \\ \omega_y''' \\ \omega_z''' \end{bmatrix} \tag{126}$$

Thus, through the Equations 123, 124, 125 and 126 and remembering that $[\omega_x''' \ \omega_y''' \ \omega_z'''] = \underline{\omega}^b_{a,b}$, the desired relation can be stated:

$$\begin{bmatrix} \frac{d\phi}{dt} \\ \\ \frac{d\theta}{dt} \\ \\ \frac{d\psi}{dt} \end{bmatrix} = \begin{bmatrix} -sin\theta & cos\theta \ sin\psi & cos\theta \ cos\psi \\ 0 & cos\psi & -sin\psi \\ 1 & 0 & 0 \end{bmatrix} \cdot \underline{\omega}^b_{a,b} \tag{127}$$

Note that this matrix is not properly a rotation matrix, because the Euler angle-rates are not orthogonal (see Figure 40). Thus, for the inverse transformation, the proper inverse of this matrix must be found (not simply transposing):

$$\underline{\omega}^b_{a,b} = \begin{bmatrix} 0 & 0 & 1 \\ \\ \frac{sin\psi}{cos\theta(sin^2\psi+cos^2\psi)} & \frac{cos\psi}{sin^2\psi+cos^2\psi} & \frac{sin\theta \ sin\psi}{cos\theta(sin^2\psi+cos^2\psi)} \\ \\ \frac{cos\psi}{cos\theta(sin^2\psi+cos^2\psi)} & -\frac{sin\psi}{sin^2\psi+cos^2\psi} & \frac{sin\theta \ cos\psi}{cos\theta(sin^2\psi+cos^2\psi)} \end{bmatrix} \cdot \begin{bmatrix} \frac{d\phi}{dt} \\ \\ \frac{d\theta}{dt} \\ \\ \frac{d\psi}{dt} \end{bmatrix} \tag{128}$$

For other Rotation sequences, the same technique can be used.

C.3. Rotation matrix definition

Rotation matrices, also called direction cosine matrices, are ways to represent a transformation between two given reference frames a and b due rotations about right-handed orthogonal set of axes. Through a rotation matrix, a vector can be transformed from a frame to another:

$$\underline{r}^b = \underline{\underline{T}}_a^b \cdot \underline{r}^a, \qquad \underline{r}^a = \underline{\underline{T}}_a^{b\ T} \cdot \underline{r}^b \tag{129}$$

Specifying a rotation θ around one given axis, the following relations describe simply rotations about this axis (planar rotations), which can be used to build more complex three-dimensional rotations:

- Around X axis:

$$\underline{\underline{T}}_1(\theta_x) = \begin{bmatrix} 1 & 0 & 0 \\ 0 & cos\theta_x & sin\theta_x \\ 0 & -sin\theta_x & cos\theta_x \end{bmatrix} \tag{130}$$

- Around Y axis:

$$\underline{\underline{T}}_2(\theta_y) = \begin{bmatrix} cos\theta_y & 0 & -sin\theta_y \\ 0 & 1 & 0 \\ sin\theta_y & 0 & cos\theta_y \end{bmatrix} \tag{131}$$

- Around Z axis:

$$\underline{\underline{T}}_3(\theta_z) = \begin{bmatrix} cos\theta_z & sin\theta_z & 0 \\ -sin\theta_z & cos\theta_z & 0 \\ 0 & 0 & 1 \end{bmatrix} \tag{132}$$

C.4. Euler Symmetric Parameters - Quaternions

C.4.1. Quaternion definition

The direction cosine matrix can be parameterized in terms of Euler symmetric parameters q_1, q_2, q_3 and q_4. They are defined as ([15]):

$$\begin{aligned} q_1 &= e_x\ sin\frac{\Phi}{2} \\ q_2 &= e_y\ sin\frac{\Phi}{2} \\ q_3 &= e_z\ sin\frac{\Phi}{2} \\ q_4 &= cos\frac{\Phi}{2} \end{aligned} \tag{133}$$

and can be regarded as the components of a quaternion.

$$\underline{q} = \begin{bmatrix} q_1 \\ q_2 \\ q_3 \\ q_4 \end{bmatrix} \tag{134}$$

Since a quaternion expresses a transformation, the notation of super and subscripts corresponds to transformation matrices. So $\underline{q}_a^b$ denotes a quaternion describing the transformation from frame a to frame b.

C.5. Relations among reference transformations

C.5.1. Euler axis-angle from Rotation Matrix

A general three-dimensional rotation matrix can be regarded as a set of Euler axis-angle $\underline{\hat{e}}, \phi$.
From the rotation matrix in Section C.5.3:

$$\phi = -arccos(\frac{1}{2}(Tr(T) - 1)) \tag{135}$$

If $sin(\phi) \neq 0$, the Euler axis is regarded as:

$$\begin{aligned} e_1 &= \frac{T_{23} - T_{32}}{2sin(\phi)} \\ e_2 &= \frac{T_{31} - T_{13}}{2sin(\phi)} \\ e_3 &= \frac{T_{12} - T_{21}}{2sin(\phi)} \end{aligned} \tag{136}$$

If $sin(\phi) = 0$, the rotation is not defined and the Euler axis can be any unity vector.

C.5.2. Euler angles from Rotation Matrix

A general three-dimensional rotation matrix can be regarded, with a specified Euler rotation sequence, into the related Euler angles (ϕ, θ, ψ).
For the example sequence 3-2-1, the rotation matrix is regarded as (see Section C.5.4):

$$\underline{\underline{T}}_{321}(\phi, \theta, \psi) = \begin{bmatrix} cos\theta\ cos\phi & cos\theta\ sin\phi & -sin\theta \\ -cos\psi\ sin\phi + sin\psi\ sin\theta\ cos\phi & cos\psi\ cos\phi + sin\psi\ sin\theta\ sin\phi & sin\psi\ cos\theta \\ sin\psi\ sin\phi + cos\psi\ sin\theta\ cos\phi & -sin\psi\ cos\phi + cos\psi\ sin\theta\ sin\phi & cos\psi\ cos\theta \end{bmatrix} \tag{137}$$

Observing the matrix above:

$$\theta = -arcsin(T_{13}) \tag{138}$$

$$\phi = atan2(T_{12}/T_{11}) \tag{139}$$

$$\psi = atan2(T_{23}/T_{33}) \tag{140}$$

where, $atan2$ is the $arctan$ function taking the signs of the matrix elements into account. It is important to note that there is an ambiguity in θ, which can be solved simply choosing $-\pi/2 < \theta \leq \pi/2$.
Further Euler rotation sequences can be obtained in the same manner, regarding an specified rotation matrix as the result of a given Euler rotation sequence. For more rotation matrices representation in function of different Euler rotation sequences, see Reference [15].

C.5.3. Rotation Matrix from Euler axis-angle

With a specified Euler axis-angle set $\underline{\hat{e}}, \phi$, a general three-dimensional rotation can be accomplished by a transformation matrix derived from this set ([15]):

$$\underline{\underline{T}}(\underline{\hat{e}}, \phi) = \begin{bmatrix} cos\phi + e_1^2(1-cos\phi) & e_1e_2(1-cos\phi) + e_3 sin\phi & e_1e_3(1-cos\phi) - e_2 sin\phi \\ e_1e_2(1-cos\phi) - e_3 sin\phi & cos\phi + e_2^2(1-cos\phi) & e_2e_3(1-cos\phi) + e_1 sin\phi \\ e_1e_3(1-cos\phi) + e_2 sin\phi & e_2e_3(1-cos\phi) - e_1 sin\phi & cos\phi + e_3^2(1-cos\phi) \end{bmatrix} \tag{141}$$

C.5.4. Rotation Matrix from Euler angles

With a specified Euler rotation sequence, and using the relations for the rotation matrices about a specified axis, a general three-dimensional rotation can be accomplished by a transformation matrix derived from the sequential multiplication of simple rotation matrices.
For the example sequence 3-2-1:

$$\underline{\underline{T}}_{321}(\phi, \theta, \psi) = \underline{\underline{T}}_1(\psi) \cdot \underline{\underline{T}}_2(\theta) \cdot \underline{\underline{T}}_3(\phi) \tag{142}$$

$$\underline{\underline{T}}_{321}(\phi, \theta, \psi) = \begin{bmatrix} cos\theta\ cos\phi & cos\theta\ sin\phi & -sin\theta \\ -cos\psi\ sin\phi + sin\psi\ sin\theta\ cos\phi & cos\psi\ cos\phi + sin\psi\ sin\theta\ sin\phi & sin\psi\ cos\theta \\ sin\psi\ sin\phi + cos\psi\ sin\theta\ cos\phi & -sin\psi\ cos\phi + cos\psi\ sin\theta\ sin\phi & cos\psi\ cos\theta \end{bmatrix} \tag{143}$$

Further Euler rotation sequences can be obtained in the same manner or from the Reference [15].

C.5.5. Rotation Matrix from Quaternion

The Rotation Matrix can be derived from a quaternion by ([15]):

$$\underline{\underline{T}}_a^b(\underline{q}_a^b) = \begin{bmatrix} q_1^2 - q_2^2 - q_3^2 + q_4^2 & 2(q_1q_2 + q_3q_4) & 2(q_1q_3 - q_2q_4) \\ 2(q_1q_2 - q_3q_4) & -q_1^2 + q_2^2 - q_3^2 + q_4^2 & 2(q_2q_3 + q_1q_4) \\ 2(q_1q_3 + q_2q_4) & 2(q_2q_3 - q_1q_4) & -q_1^2 - q_2^2 + q_3^2 + q_4^2 \end{bmatrix} \tag{144}$$

C.5.6. Quaternion from Rotation Matrix

From rotation matrix diagonal elements (see Equation 144), it is possible to realize that there are 4 different ways to get the quaternion components from the rotation matrix elements. All the 4 ways are mathematically equivalent, but numerical inaccuracies can be minimized by avoiding calculations in which the quaternion component appearing in the denominator is close to zero.
Hence, from the diagonal elements it is possible to retrieve the quaternion component absolute values and these values must be analyzed in order to get the biggest one, to be used as reference, in order to retrieve its other related components.

Thus, there are 4 possible calculation combinations:

•q_1 as reference:

$$\begin{bmatrix} q_1 \\ q_2 \\ q_3 \\ q_4 \end{bmatrix} = \begin{bmatrix} \frac{\sqrt{1+T_{11}-T_{22}-T_{33}}}{2} \\ \frac{T_{12}+T_{21}}{4q_1} \\ \frac{T_{31}+T_{13}}{4q_1} \\ \frac{T_{23}-T_{32}}{4q_1} \end{bmatrix} \tag{145}$$

•q_2 as reference:

$$\begin{bmatrix} q_1 \\ q_2 \\ q_3 \\ q_4 \end{bmatrix} = \begin{bmatrix} \frac{T_{12}+T_{21}}{4q_2} \\ \frac{\sqrt{1-T_{11}+T_{22}-T_{33}}}{2} \\ \frac{T_{23}+T_{32}}{4q_2} \\ \frac{T_{31}-T_{13}}{4q_2} \end{bmatrix} \tag{146}$$

•q_3 as reference:

$$\begin{bmatrix} q_1 \\ q_2 \\ q_3 \\ q_4 \end{bmatrix} = \begin{bmatrix} \frac{T_{31}+T_{13}}{4q_3} \\ \frac{T_{23}+T_{32}}{4q_3} \\ \frac{\sqrt{1-T_{11}-T_{22}+T_{33}}}{2} \\ \frac{T_{12}-T_{21}}{4q_3} \end{bmatrix} \tag{147}$$

•q_4 as reference:

$$\begin{bmatrix} q_1 \\ q_2 \\ q_3 \\ q_4 \end{bmatrix} = \begin{bmatrix} \frac{T_{23}-T_{32}}{4q_4} \\ \frac{T_{31}-T_{13}}{4q_4} \\ \frac{T_{12}-T_{21}}{4q_4} \\ \frac{\sqrt{1+T_{11}+T_{22}+T_{33}}}{2} \end{bmatrix} \tag{148}$$